THE GEOLOGY, PETROLOGY AND CONTROLS ON COPPER MINERALISATION IN EXPLORATION PROSPECTING LICENCE (EPL) 5836 ALONG THE MATCHLESS BELT, WINDHOEK, NAMIBIA.

Submitted by

Halleluya-Naantu Ekandjo

906220

A Research Report submitted to the Faculty of Science, University of the Witwatersrand, in partial fulfilment of the requirements for the degree of Master of Science.

February 2017

Supervisor: Prof. Paul Nex

Declaration

I declare that this research report is my own, unaided work. It is being submitted for the Degree of Master of Science at the University of the Witwatersrand, Johannesburg. It has not been submitted before for any degree or examination at any other University.

Halleluya-Naantu Ekandjo

27th February 2017 in Johannesburg

Abstract

The Kariam Prospect mineralisation is a quartz-carbonate vein hosted Cu (Mo-Au) deposit associated with quartz-carbonate schist and biotite-chlorite schist of the Kuiseb Formation in the Southern Zone or Khomas Trough of the Damara Orogen in Namibia. Geological mapping within the 'Northern Part' of the Kariam Prospect has identified two different types of schists which are different in composition and different in outcrop appearance, namely the fine-grained mica-rich and medium-grained quartz-rich schist. They dip shallowly between 15° - 55° towards 220° - 320° and strike ENE-WSW. They were originally sediments deposited around 630 Ma during the Neoproterozoic. Two different sets of veins have been noted around the schists reflecting different hydrothermal activities which have taken place in the area. The veins are i) Quartz-carbonate magnetic veins dipping steeply at 80° SE, estimated to have formed after deformation and ii) Quartz non-magnetic veins parallel to the schistosity with a steep dip inferred to have formed during deformation. A petrographic and borehole core investigation revealed that the different types of schists exhibit a different mineralogy attributed to alteration. Mineralisation in the form of chalcopyrite, pyrite, pyrrhotite and molybdenite occurs as disseminated ore, patches, blebs, and veinlets within the veins and matrix of the host rocks proximal to the mineralised veins. Adjacent alteration comprises proximal quartz-carbonate and early/distal biotite chlorite zoned clusters.

Acknowledgement

I would like to express gratitude to Prof. Paul Nex for his supervision, guidance, patience and willingness to review my work. Special thanks to Prof. A.F Kamona for getting me this project. I would be in debt if I don't mention Mr Basie for his support during my field work, thank you for showing me all roads and for driving me to the field when I didn't have a 4x4. Acknowledgments are owed to DAAD for partly funding my research, you made it all possible.

I am grateful to the Geological Survey of Namibia for allowing access to drill core and samples collection. A special thanks to Dr Branko Corner for providing me with existing reports and data.

I would like to thank my family for their love, support and encouragement. Thanks mom and dad for believing in me. Finally, I would like to thank my siblings and friends for keeping me motivated and telling me things will be alright when I felt like giving up.

Table of Contents

List of Figures

List of tables

Abbreviations

EPL: Exploration Prospecting License

FVD: First Vertical Derivative

GSN: Geological Survey of Namibia

MAB: Matchless Amphibolite Belt

MAM: Matchless Amphibolite Member

MRS: Mica-rich schist

PPL: Plane Polarised Light (in petrology)

QRS: Quartz-rich schist

RTP: Reduced to the Pole

SZ: Southern Zone

VMS: Volcanic Massive Sulphides

XPL: Cross Polarised Light (in petrology)

CHAPTER 1

INTRODUCTION

Exploration and exploitation of mineral deposits especially metalliferous ones, is vital for many developing countries to sustain their economic development. Metals such as copper, nickel and zinc are still required to support and maintain fast-growing industrial development. Finding new mineral deposits and having a better understanding of the existing deposits is important and necessary for developing countries to sustain their economy, thus this thesis focuses on determining the lithological and structural controls of copper mineralisation in Exploration Prospecting License (EPL) 5836, approximately 10 km north of the Matchless Amphibolite Belt, Namibia.

1.1 Background

Copper has been one of the most important commodities in Namibia with a wide range of different deposit styles (Miller, 1983; Schneider and Seeger, 1992). Some of these deposits include platform carbonate-hosted mineralisation of the Tsumeb and Kombat Mines at approximately 530 ± 11 Ma, the Volcanogenic Massive Sulphide (VMS) deposits of the Matchless Amphibolite Belt in the Southern Zone of the Damara Belt and the Kalahari Copper Belt that stretches for over 800 km from central Namibia into northern Botswana (Klemd, 1987). This project focuses on the mineralisation approximately 10 km north of the Matchless Amphibolite belt of the north-east arm of the Damara belt aimed at understanding the stratigraphy and the controls of mineralisation.

1.2 Location of the study area and land ownership

The study area is located within the central part of Namibia, approximately 70 km south-west of the capital city Windhoek (Fig 1.1). More specifically, it is situated about 40 km southwest of the Matchless Mine and is within the Farms Kariam and Sonderwater in the Khomas region. Access is made from the C28 road from Windhoek and farm private roads. Geologically the area is located within the Southern Zone of the Damara belt (Fig 1.2) and it is dominated by the Kuiseb Formation schists. It is owned by Zender Minerals Investments, previously owned by Kuiseb Copper Company (Pty) Ltd. The study area is demarcated with the red block (Fig. 1.1) and labelled as Exclusive Prospecting License (EPL) 5836 (Fig. 1.2).

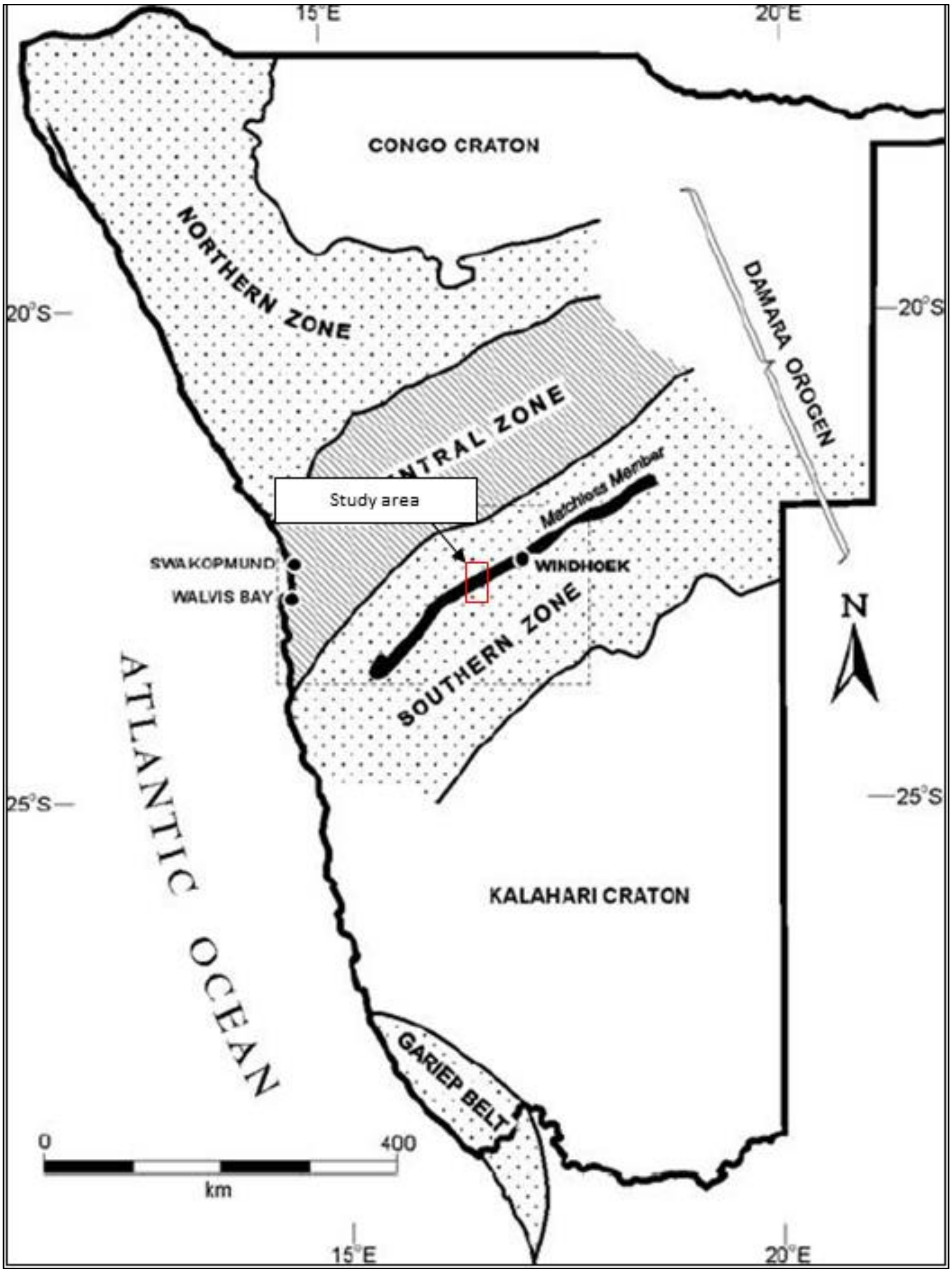

Figure 1.1: Locality map showing the Matchless Member and area of study within the Southern Zone of the Damara Orogen, approximately 10 km north of the MAB, see figure 1.2 for a more detailed locality map.

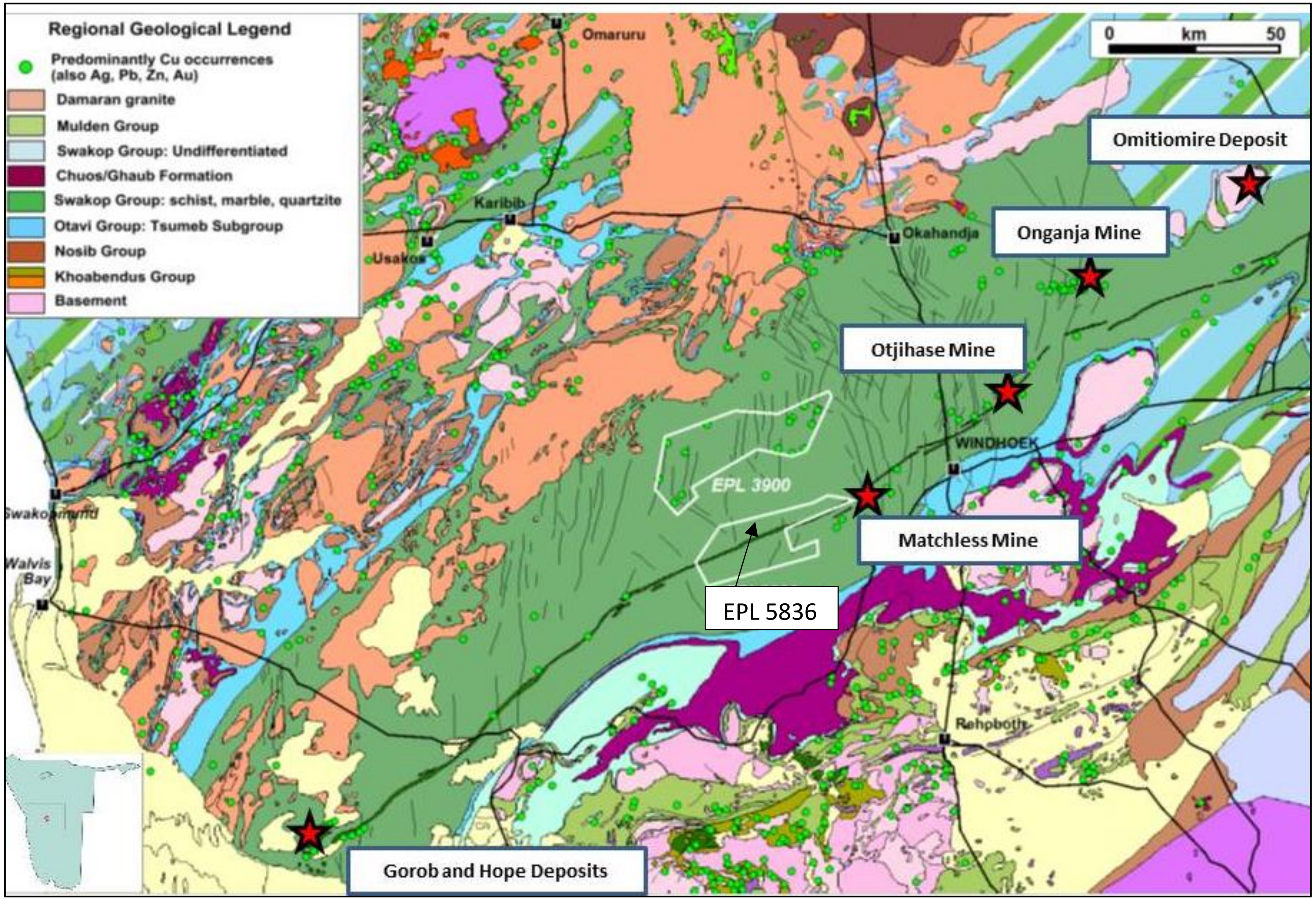

Figure 1.2: A detailed regional geological map of the central portion of the Damara Belt, modified from Kuiseb Copper Company (2013). The Matchless Amphibolite Belt (MAB) is shown by a discontinuous solid black line and the study area is indicated by the black arrow, about 10 km north of the MAB is labelled EPL 5836.

1.3 Statement of problem

The geology in EPL 5836 is poorly understood and the controls of the mineralisation in the area have not been identified, therefore this research will mainly focus on determining the structural features that control the mineralisation in relation to the geology of the area.

1.4 Aim

This research is aimed at establishing the structural and stratigraphic controls of the copper mineralisation observed in the study area with respect to the local geology. Some of the objectives that will be addressed include: establishment of a detailed stratigraphy from traverses. It is thought that the structural controls of the vein-hosted copper mineralisation in EPL 5836 are related to one or more deformation phases of the Damara Orogen which resulted in fluids depositing the copper and gold in veins.

1.5 Methodology

The objectives of this research were achieved through the following activities; desktop studies, field work including borehole core logging and geological mapping, sampling, and petrographical studies. Prior to field work, a review of previous work was carried out to understand the geology, structures and mineralisation within the belt to establish relationships between the known deposits and the obtained data.

Detailed logging of two existing boreholes was carried out based on lithological intervals as well as alteration zones. Structural features were noted and described, and occurrences of mineralization were examined in detail. Structural and stratigraphic controls of mineralisation were investigated. Additionally, alteration and subsurface lithologies were determined. Six samples were submitted for polished thin sections prepared at the University of the Witwatersrand to help in identifying the mineralogy and associated micro-structures.

Geological mapping was conducted for a week on the farms Kariam and Sonderwater to establish the local geology and to determine the stratigraphic sequence and structural features and noting evidence for mineralisation. In addition, representative rock samples were collected for thin sections which were prepared at the University of Namibia. Garmin eTrex 30 GPS, compass, hammer and base maps were used during field work. Research ethics were maintained by obtaining necessary permission from the land and EPL owners for access and minimal damage to the environment. Four samples were submitted at the University of Namibia for thin sections.

Data collected during field work were transformed into geological traverses. An ortho-photo was used as base map however the local vegetation obscured the outcrops. ArcGIS, and Google Earth Pro were used to compile the information from two traverses.

Where practically possible, unweathered representative samples were collected of all lithologies encountered. Four rock samples collected during field work were submitted to the University of Namibia for thin sections and 6 core samples were transported to The University of the Witwatersrand after being granted an export permit.

CHAPTER 2

GEOLOGICAL SETTING

2.1 Regional geological setting

During the Mesoproterozoic, the amalgamation of several continental fragments formed the supercontinent Rodinia, with orogenic belts marking the suture zones between these fragments (Hoffman, 1991; Miller, 2008). At about 850 Ma, rift valleys formed during the break-up of Rodinia which led to the splitting of Antarctica and Africa from South America (Miller et al., 1983). Large rivers flowed into valleys, depositing sediments, and saline lakes formed much like those present in the East African Rift Valley today. The Adamastor and Khomas oceans were subsequently created as the land masses continued moving apart (Miller et al., 1983). At about 700 Ma these land masses once again started moving together, the fragmentation and reshuffling was followed by the renewed amalgamation to form the supercontinent Gondwana at approximately 550 Ma (Miller, 2008).

Near the end of the Neoproterozoic, Namibia formed part of Gondwana and was located at a triple junction between the Adamastor Ocean separating the Congo-(Angola) and the Kalahari cratons from the Rio de la Plata and Amazon cratons and the northeast trending Damara Belt between the Congo and Kalahari cratons (Gray et al., 2008) (Fig. 2.1). This Pan African compression resulted in the closure of both the Adamastor Ocean and Khomas Sea. The closure of the Adamastor Sea resulted in the formation of the Kaoko Belt in northern Namibia and the formation of the Gariep Belt in the south of Namibia, while the closure of the Khomas Sea (Matchless aulocogen) resulted in the formation of the Damara Belt, the north-east trending intracontinental branch (Fig.2.1) (Gray et al., 2008). The area of study is within the southern part of the Damara Belt.

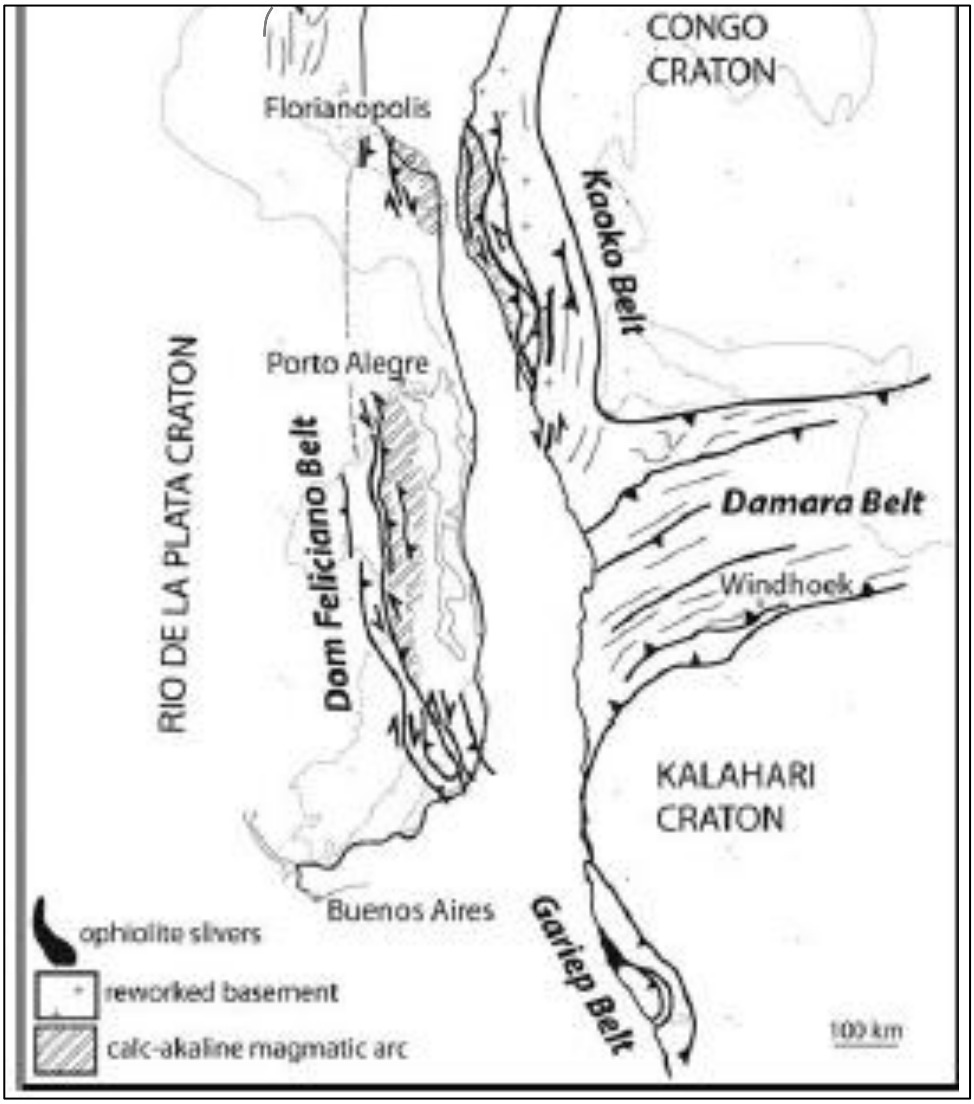

Figure 2.1: Map of Pan-African Orogen with the orogenic system made up of different belts; Kaoko Belt, Gariep Belt and the inland Damara Belt and cratons; the Kalahari and Congo Cratons. The ocean separating the Kalahari-Congo Craton from the Rio de la Plate Craton corresponding to the Adamastor Ocean and the Khomas Sea occupying the area labelled the Damara Belt, modified from Gray et al., (2008).

The Damara Orogenic Belt which strikes ENE across the central and northern Namibia (Fig. 2.1 and Fig. 2.2) is part of the early Palaeozoic to late Precambrian Pan African network of orogenic belts (Downing and Coward, 1981), and it contains thick sequences of Neoproterozoic sediments that rest unconformably on Mesoproterozoic basement (Miller, 2008). It chronicles the high-angle convergence and the closure of the Khomas Sea ocean between the Congo and Kalahari cratons in the latest Neoproterozoic and early Phanerozoic (Miller, 1983). This east-northeast arm is divided into several distinct zones based on stratigraphy, structure, metamorphic grade, plutonic rocks, geochronology and aeromagnetic expression (Breitkopf and Maiden, 1988; Miller, 1983, 2008). Miller (1983) referred these tectonostratigraphic zones as the Northern Platform (NP), Northern Zone (NZ), Central Zone (CZ), Okahandja Lineament Zone (OLZ), Southern Zone (SZ), Deep-Level

Southern Zone, Southern Margin Zone (SMZ) and the Southern Foreland (SF) (Fig. 2.2 and Fig. 2.3) and this study concentrates on the Southern Zone.

The depositional, metamorphism and deformational evolution of the central Damara orogeny is complex, and Miller (1983) summarised it as extensional-rifting-spreading and compressional-convergence-collision phases, which ultimately led to the development of a metamorphic belt known as the Matchless Amphibolite Belt (MAB) within the Southern Zone.

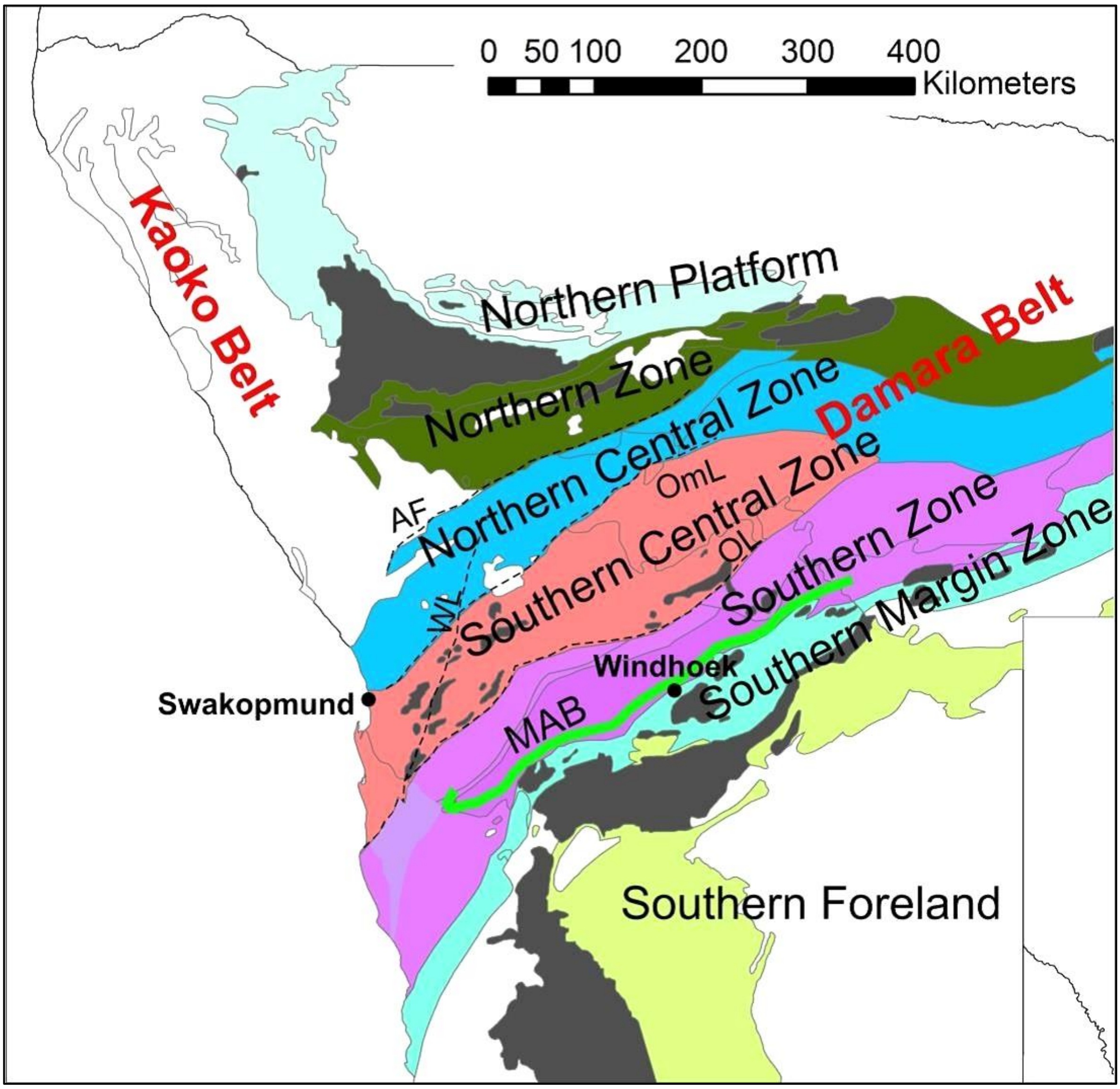

Figure 2.2: Simplified geological map of the Damara Belt showing the main tectonostratigraphic zones. The green solid line represents the Matchless Amphibolite Belt (MAB), modified from Miller (1983).

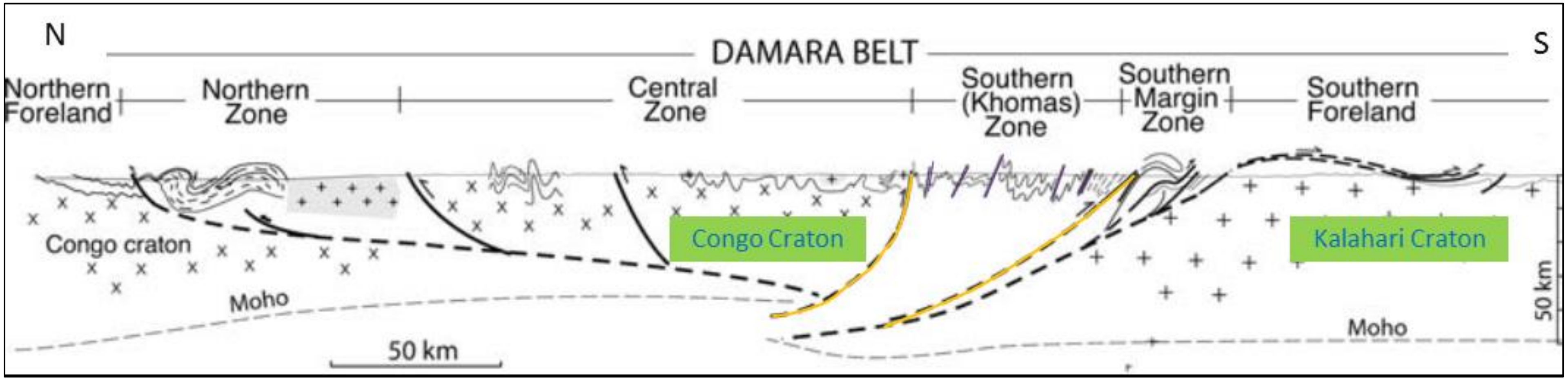

Figure 2.3: Geological profile showing the crustal architecture of the Damara Belt of the Damara Orogen, also showing the tectonostratigraphic zones within the Damara Belt (Gray et al., 2008). The tectonostratigraphic area of interest, the SZ is highlighted in orange, with all the structural features within it (MAB is within the SZ).

2.2 Local geology of the Southern Zone

The Southern Zone also referred to as Khomas Zone or Khomas Trough formed a second NE-trending, deep-water branch during extension known as the Khomas Sea (Miller, 2008). It is the only region in the Damara Belt where the continental breakup and the development of the ocean floor took place, with the subduction of it beneath the Central Zone leading to the collision of the Congo and Kalahari Cratons (Fig. 2.3) (Kukla and Stanistreet, 1991; Miller, 2008). It forms the deeply eroded accretionary prism of the belt, underlain by a thick sequence of meta-turbidites, with south-to southeast-vergent folding and thrusting of the Kuiseb Formation which records off-scraping, underplating and burial of originally trench sediments during the north or north-westward subduction of the Kalahari below the Congo craton at about 580-520 Ma (Fig. 2.3) (Kukla, 1992; Miller, 2008).

According to Miller (2008), the Southern Zone prism is adjacent to the magmatic arc of the Central Zone along the Okahandja Lineament Zone, while in the south it structurally overlies the shallow dipping older rocks of the Southern Marginal Zone foreland which is part of the under-thrusted Kalahari Craton. The Southern Zone is a low temperature-high pressure zone containing both passive margin and active margin schist successions (Kukla, 1992; Miller, 2008), with the spreading schists forming part of the Kuiseb Formation and the overlying active-margin schists placed in the Hureb Formation by de Kock (1989).

Within the Southern Zone, the Matchless Amphibolite Belt (MAB) occurs as a narrow linear unit (0.5-3 km wide) (Breitkopf and Maiden, 1988; Klemd et al., 1989; Miller, 2008), extending in a north-easterly direction traceable over nearly 400 km from a point 100 km south-east of Walvis Bay, through Windhoek to Steinhausen, beyond which it is hidden by surficial cover (Kukla, 1992; Killick, 2000). The chemical composition of the amphibolite member is composed of metabasic rocks of mid-oceanic ridge basalt (MORB) (Barnes and Sawyer, 1980; Miller, 1983; 2008), which suggests a rift environment with minor continental flood basalts (Barnes and Sawyer, 1980). The Matchless Member is hosted in the Kuiseb schists and formed above a sediment-covered mid-oceanic ridge in the Khomas Sea (Miller, 1983, 2008; Breitkopf and Maiden, 1986).

2.3 Stratigraphy of the Southern Zone

The Damara belt is divided into four groups, namely the Nosib Group which is the oldest, Swakop Group, Otavi Group and a molasse known as the Nama Group, with only the Swakop Group represented in the Southern Zone (Miller, 2008). Most of the SZ comprises Kuiseb schists, which are overlain by locally developed, syntectonic arc trench metagreywackes of the Hureb Formation (Kukla, 1992; Miller, 2008).

The Matchless Amphibolite Member (MAM) within the belt is part of the Kuiseb Formation, forming the uppermost stratigraphic unit of the Swakop Group (Table 1) (Miller, 1983; Killick, 2000). The

Kuiseb Formation is comprised of an argillaceous assemblage of quartz-mica schists with minor carbonaceous schists and calc-silicates (Table 1) Killick (2000), which are interbedded with amphibolite and amphibolite schists of the Matchless Member (Breitkopf and Maiden, 1988; Killick, 2000). Schneider (1983) believes that the schists of the Kuiseb Formation were initially pelites, feldspathic siltstones and sandstones while Miller (1983) and Kukla (1992) believe that they were greywackes.

Most importantly, there are no reliable ages for the Matchless Member. An Rb-Sr age of 765 ±37 Ma was obtained by Hawkesworth et al (1981) which they suggested as the minimum emplacement age of the Matchless Member. An approximate emplacement age of 635 Ma was obtained by Frimmel et al (2011) from the Kuiseb Formation schists.

Table 1: The stratigraphy of the Damara Sequence in the southern part of the Damara Belt of the Damara Orogen (Killick, 2000). The red lines outline the stratigraphy present in the Southern Zone..

Group	**Sub-group**	**Formation**	**Lithology**
Swakop	Khomas	Kuiseb	Quartz-mica schist with minor intercalations of carbonaceous schist and amphibolite (Matchless Member within the MAB)
		Auas	Quartzite, schist, dolomite and amphibolite
		Chuos	Mixtite, schist, amphibolite and itabirite
	Kudis		Dolomite, mica schist, carbonaceous schist and quartzite
Nosib			Quartzite, phyllite and conglomerates

2.4 Deformation and metamorphism history of the Southern Zone

The SZ is characterised by three main deformation phases (D_1 to D_3) with a weak D_4 only occurring in the southern part of the SZ (Miller, 2008). Schists of the Kuiseb formation were affected by all four deformational phases. The collisional event termed the Khomas Orogeny is noted to have produced the progressive D_2 as well as the D_3 fold and thrust phases of deformation in the Southern Zone of the main Damara Orogen (Coward, 1983; Kukla et al., 1988; Kukla, 1992).

D_2 is generally the main folding phase which accounts for the development of the observed isoclinal, metre-scale folding, thrusting with an overall vergence to the southeast in the vicinity of the Matchless Belt and the northwest-dipping S_2 cleavage (Fig. 2.3) (Breitkopf and Maiden, 1988; Kukla et al., 1988; Miller, 2008). D_3 folds within the SZ are upright and open south of the OL and they become south-east vergent and isoclinal southwards (Miller, 2008).

The intensity of deformation is observed to increase southward across the Southern Zone (Breitkopf and Maiden, 1988) and the continued thrusting and crustal thickening in the Southern Zone is believed to be due to the major south-directed bulk shear strain deformation (Fig.2.3) (Gray et al., 2008). In addition, Miller (2008) suggested that all structures within this vicinity become SE vergent and isoclinal toward the southeast, with all the older structures so intensely overprinted by younger structures that only a single part, NW-dipping, bedding-parallel foliation can be recognized. Furthermore, deformation in the SZ is dominated by a fabric/foliation as noted by Moore (2010) and this fabric includes elements of primary bedding and two early foliations parallel to the recumbent deformational events (Miller, 1983).

The Kuiseb Formation of the Southern Zone is comprised of sediments and minor volcanic extrusions that accumulated in an extensional marine basin (Killick, 2000). Klemd et al. (1989) proposed that major porphyroblastic mineral growth took place after D_2 at amphibolite facies metamorphic grade (temperature of 550-625^{0}C and pressure of 6-8 Kbar) which Kasch (1983) referred to kyanite metamorphism (Fig. 2.4).

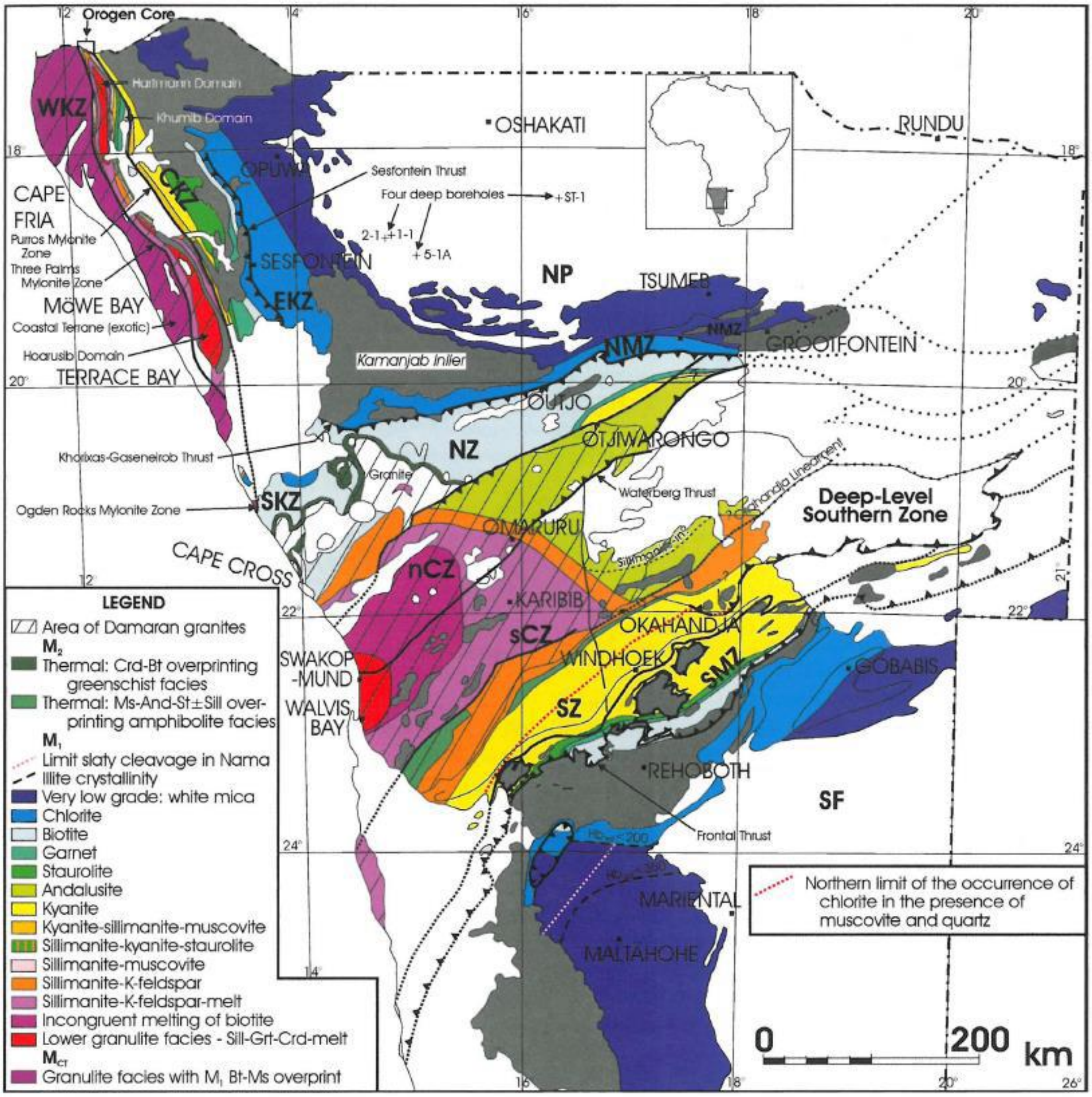

Figure 2.4: Metamorphic zones for semi-pelitic and pelitic rocks in the Damara Orogen. The study area is located within the Kyanite zone of the SZ (from Miller, 2008).

2.5 Mineral Deposits of the Matchless Belt

The mineral deposits within the Matchless Belt are described as volcanogenic-massive sulphide (VMS) deposits with remnants of a primary structure (Killick, 2000). There are about 18 known base metal deposits along the Matchless Amphibolite Member (MAM) which have been grouped into four clusters known as the Gorob, Niedersachsen, Matchless and Otjihase Clusters (Fig. 2.5). Known deposits within this belt include Matchless, Otjihase, Hope, Gorob and Onganja which are mainly stratiform cupriferous pyrite deposits, with subordinate but variable amount of lead, silver and gold. Most of the mineralisation within the vicinity of the amphibolite belt is associated with banded and/or massive tabular magnetite quartzite and it occurs as hairline fractures, veinlets or sulphide-bearing quartz-carbonate veins referred to stringer veins (Killick, 1982). Klemd et al. (1987) noted that the Matchless sulphide deposits are characterised by an abundance of -pyrite, pyrrhotite, chalcopyrite, sphalerite with minor cubanite and molybdenite. Killick (2000) observed a close association of these deposits with the Matchless Member (Fig. 2.5).

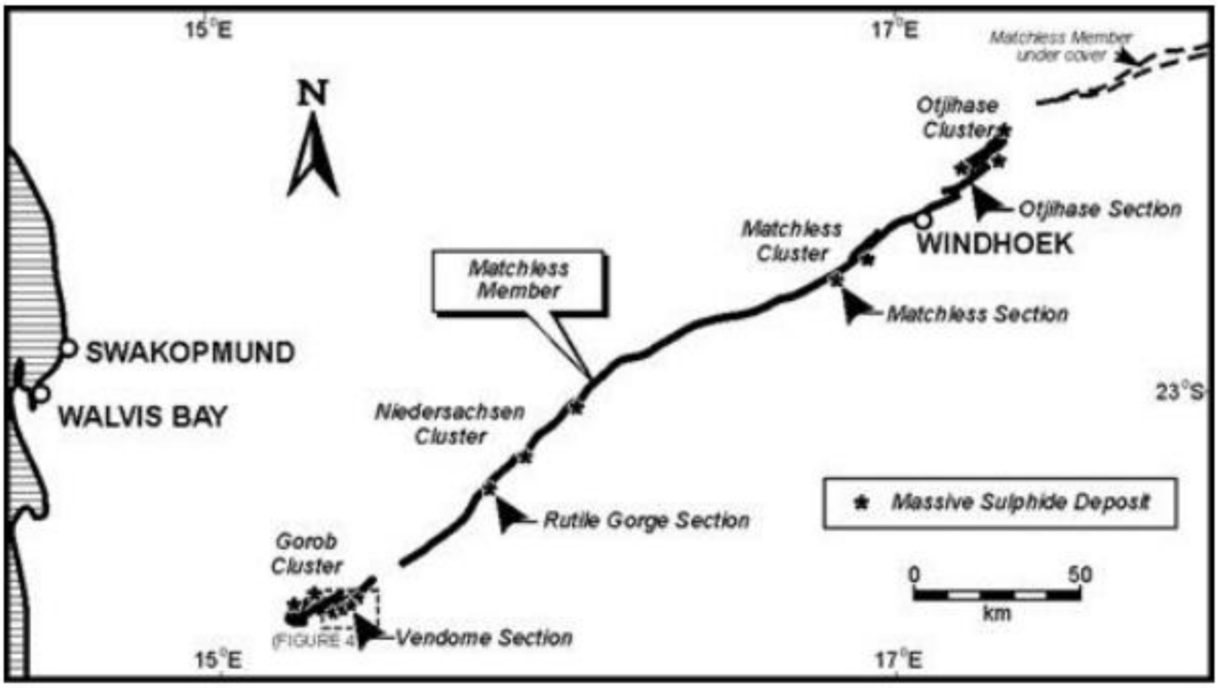

Figure 2.5 Simplified map showing the distribution of the base metal VMS sulphide deposits associated with the Matchless Member (Killick, 2000).

At the Matchless Mine the metal deposits are in close vicinity to the amphibolite but are generally hosted by amphibolites and quartz-sericite schists. The ore-grade mineralisation is not restricted to a specific rock type but is hosted by quartz-muscovite-pyrite schist, magnetite quartzite, chlorite-amphibolite-ankerite schist, amphibolite schist and massive sulphide rock as clarified by Maiden (1993). Furthermore, most schist and some sulphide-bearing rocks possess a fine layering parallel to the major lithological layering, possibly bedding (Klemd et al., 1987).

The ore is rich in chalcopyrite with varying amounts of pyrrhotite and sphalerite and these sulphides are associated with schist, magnetite quartzite and quartz-carbonate veins (Klemd et al., 1987). Sulphide-bearing quartz and carbonate veins are observed by Klemd et al. (1987) to have developed in several structural positions such as in chloritic schists and banded pyritic ore which occur as boudins within the planes of S_2 cleavage and as clasts within fragmental ore. Additionally, these sulphide veins occur in the fragmental ore which is concentrated along the interfaces between sulphide rock and hanging wall amphibolite in the River shoot and at the extremities of sulphide cusp structures (Klemd et al., 1987). Sulphide-rich rocks in the Matchless mine are affected by brittle fracture and brecciation which are healed by quartz-carbonate and pyrite to marcasite alteration (Klemd et al., 1987).

At Otjihase Mine, the deposit occurs close to Matchless amphibolite member in a monotonous sequence of quartz-mica-garnet schist of the Kuiseb Formation. There are four sub-parallel spatula-shaped mineralised shoots, namely the main shoot 2, shoot 3 and shoot 4. All the shoots occur approximately on the same stratigraphic level and are separated by more than 100 m of quartz-mica schist country rocks (Breitkopf and Maiden, 1987).

Table 2: Shows the metal deposits associated with the Matchless member of the Southern Zone, after Breitkopf and Maiden (1987), Klemd et al. (1987) and Killick (2000).

Deposits	**Size of Deposit**						**Shape of Ore Body**			**Host Rocks**
	Tonnes x 10^6	**Averange Thickness (metres)**	**Commodities**				**# of Shoots**	**Average Plunge and Dip**		
			% Cu	***% Zn***	***g/t Ag***	***g/t Au***		***Plunge***	***Dip***	
Ongombo	3	1.6	1.9	0.00 1-0.1			4			Quartz-biotite-chlorite-schist, Massive & Semi- massive sulphides & Magnetite Quartzite
Otjihase	16	2.5	2.2	0.3	12	1.2	3	6^0 W	16^0 NW	Massive & Semi- massive sulphides, Magnetite Quartzite, Actinolite-sulphide-magnetite rock.
Matchless	3.0	1-10	2.2		10-20	0.5-1.5	4		40^0 NW	Massive & Semi- massive sulphides, Sericite-quartz schist, Mica schist, amphibolite schist, amphibolite.
Gorob	1.8	3.6	2.4				8			

Another interesting deposit within the SZ is the Onganja deposit, located 65 km north-east of Windhoek. It is hosted by quartz-biotite-plagioclase schists of the Kuiseb Formation, with zones of mineralisation (Moore, 2010). It is stated in Moore (2010) that the mineralisation is in the form of vein hosted chalcopyrite and is restricted to the elongated domal structure, trending WNW. Futhermore, Onganja is described to be genetically unrelated to the syngenetic massive-sulphide copper deposits of the Matchless Belt, however there are similarities in metal associations (pyrite-chalcopyrite-magnetite and minor gold) with the Otjihase and Matchless mines (Moore, 2010).

CHAPTER 3

GEOLOGICAL FIELD WORK

During a period of 5 days from the 21st May -25th May 2016, field work in the form of geological mapping and sample collection was undertaken on the farms Sonderwater and Kariam. Before any mapping/ work was done, a day was spent with Mr. Basie, the owner of farm Sonderwater examining all the roads and the areas visited by the previous drilling group. Due to insufficient previous data, two areas of interest (Fig. 3.1) were identified from a map obtained from the company's presentation for 2013 complied by Branko Corner (Fig. 3.2, 3.3 and 3.3). Seven transects were carried out to examine the local geology (Fig. 3.1 and Fig. 3.4). The lithologies identified were named based upon visible mineralogy and colour of both weathered and unweathered surfaces. There is little outcrop (~20 %) and most of the area is covered by vegetation and sand.

The local lithologies comprise of Kuiseb Formation schists. Two different types of schists striking approximately ENE-WSW were observed;

i. a competent, dark grey quartz-rich schist and

ii. a greenish fine-grained mica-rich schist with a uniform foliation and a NW dip. This contains a speckled medium grained schist associated with the late quartz veins.

Additionally, two phases of quartz veining are evident;

i. quartz veins parallel to the regional lithological foliation and

ii. late-tectonic quartz veins at an oblique angle to the regional lithological foliation striking NNE-SSW.

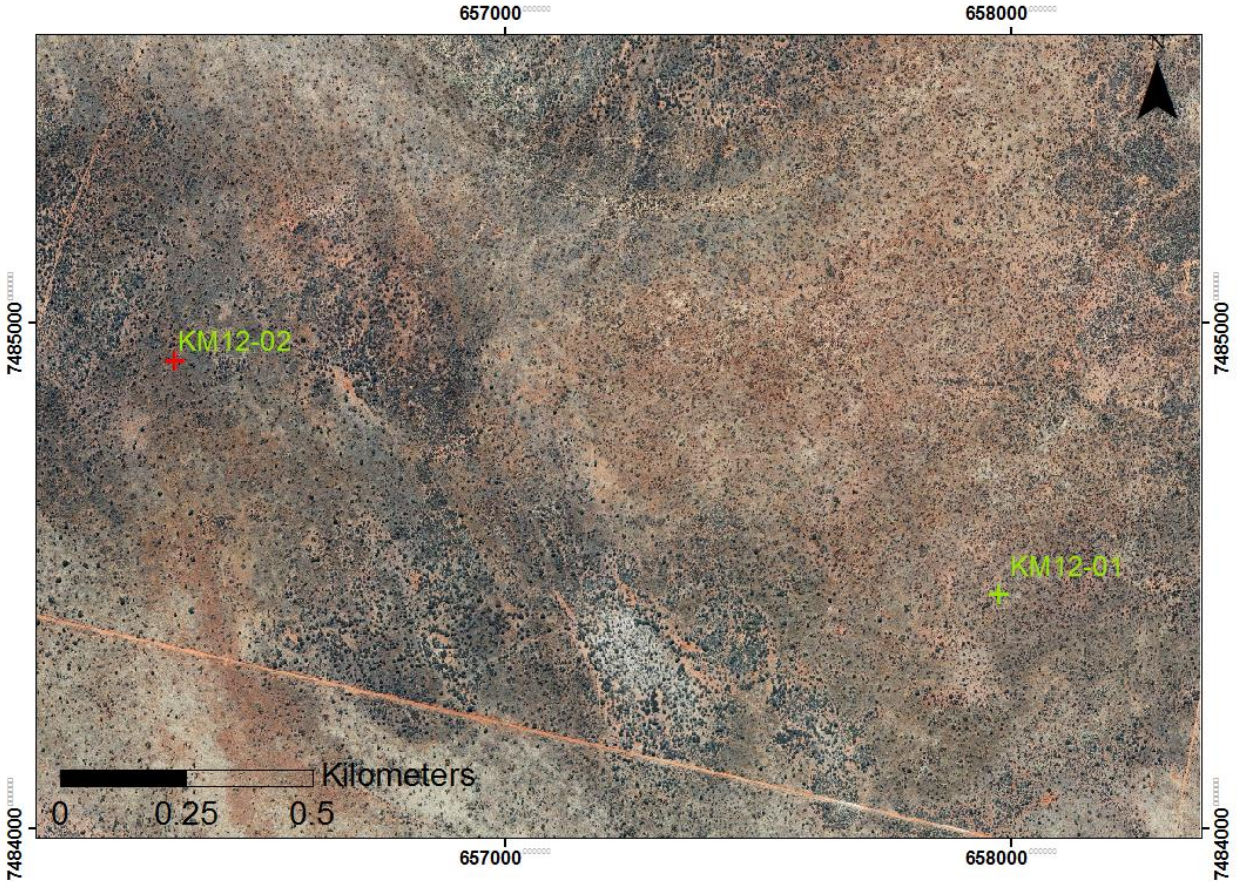

Figure 3.1: Ortho-photograph over the Kariam Prospect. The green and red crosses correspond to borehole positions of KM12-01 and KM12-02 respectively.

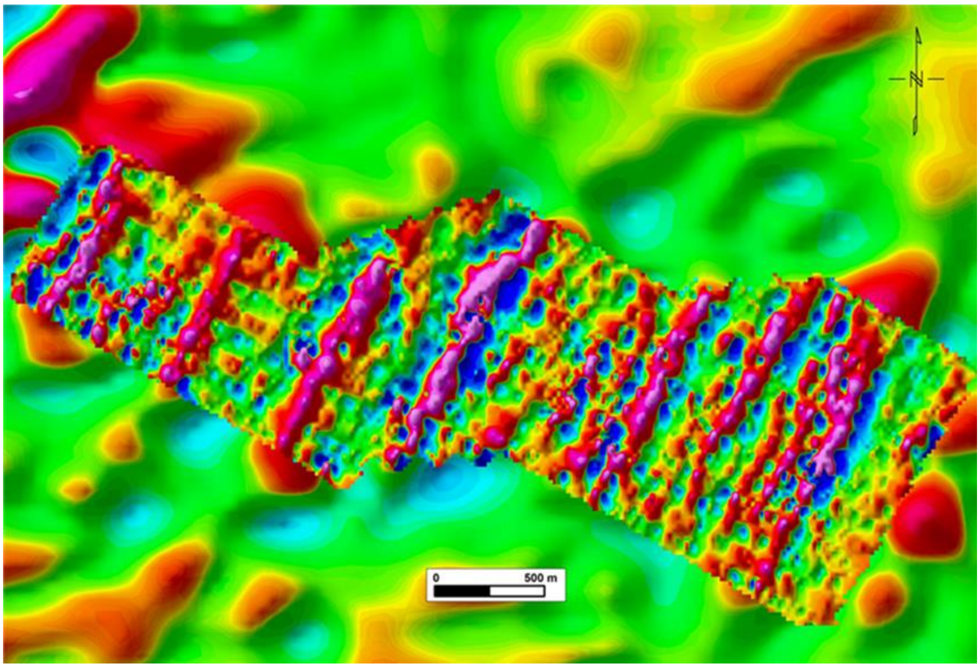

Figure 3.2: First vertical derivative (IVD) of the ground RTP magnetic data overlain on the GSN IVD (100m NW and 200m NS line spacing respectively) (Kuiseb Copper Company, 2013).

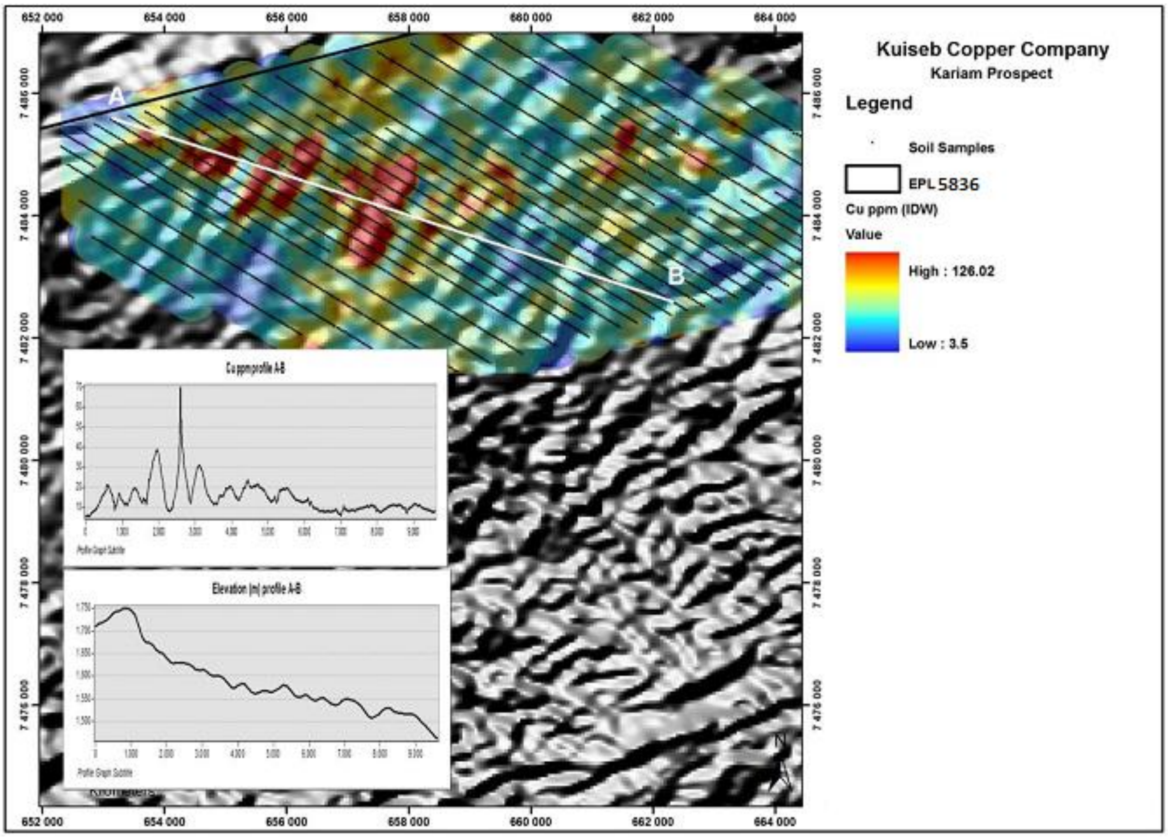

Figure 3.3: Gridded Cu values overlaid on the sun-shaded DTM image. The Cu and elevation profiles along section A-B shows the highest Cu anomalism direction (Kuiseb Copper Company, 2013).

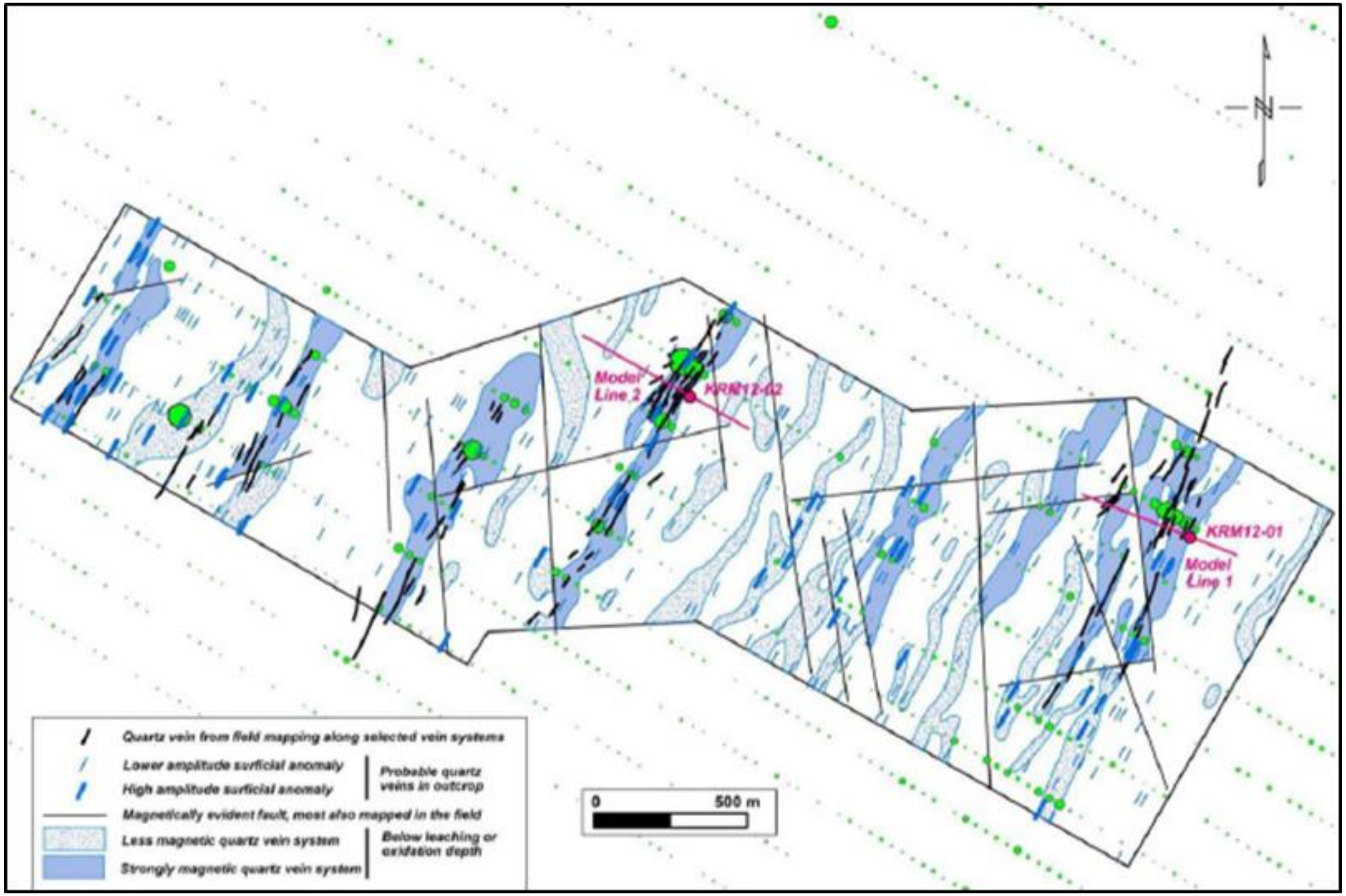

Figure 3.4: Field mapping and interpretation of ground magnetic data. The green dots represent copper values within the largest sized symbol represent high copper values. The pink lines show the modelled sections and drill hole collars (Kuiseb Company Copper, 2013).

EPL 5836 hosts the Kariam copper anomaly which is a geophysical anomaly consisting of 14 NNE-SSW individual magnetic anomalies which resulted from highly gossanous quartz veins with associated or proximal magnetite (Fig. 3.2, Fig. 3.3 and Fig. 3.4) (Kuiseb Copper Company, 2013). Two diamond drillholes were drilled after carefully studying the magnetic and soil data (see positions of drillholes in Fig. 3.1 and Fig. 3.4).

The black discontinuous lines in figure 3.4 represent quartz veins located from field mapping by Kuiseb Copper Company (2013) striking NNE, a similar orientation was obtained from the recent field mapping for this thesis. The dark and light blue linear pockets represent strongly magnetic quartz and less magnetic quartz vein systems respectively obtained from the ground magnetic data produced by the Kuiseb Copper Company (2013). The quartz veins parallel to foliation are not visible from the magnetic data provided. The green proportional symbols (dots) represent the copper values from soil samples with the largest dots representing the highest copper grade obtained.

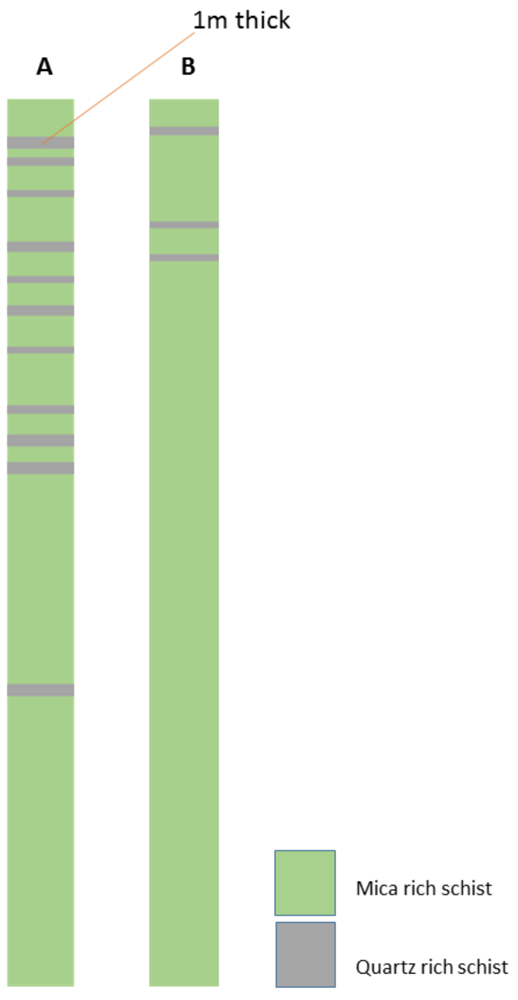

Figure 3.5: Simplified geological transects completed across the Kuiseb schist in areas of KM12-01 (A) and KM12-02 (B), see position of transects in figure 3.1. Area of study is dominated by the recessive, intensely foliated mica schist intercalated with layers of the Quartz-rich schist. The sections have been arranged from southwest on the right to north-west on the left. Refer to figure 3.1 for the locations of the sections.

The mica-rich schist dominates the area of study, intercalated with the competent, rarely foliated, massive quartz-rich schist. Quartz veins are observed parallel to and cross cutting the foliation of the mica-rich schist and none were identified close to the quartz-rich schist. The locations of the sections are indicated in Figure 3.1 and reproduced in a simplified form in Fig 3.5. The thicknesses of the two identified units differ along the length of the sections. A speckled feature is observed close to all veins that cross-cuts the lithological foliation of the mica-rich schist.

Quartz-rich schist (QRS)

This generally has dark brown surfaces due to weathering and oxidation but preserves the medium grey colour on fresher parts. It is medium-grained with little or no foliation. It is comprised mostly of quartz with minor biotite. It is a competent unit, makes up the topographic highs and can be seen very well striking ENE-WSE from a distance (Fig.3.6). The quartz-rich schist contains very minor thin and broadly spaced quartz veins. Most of the schists occur as boulders around sites of outcrops (Fig. 3.6). It is interbedded with the more recessive greenish fine-grained mica-rich schist and few clear contacts were identified. No mineralisation was observed within the unit.

Figure 3.6: Field photographs of the quartz-rich schist of the Kuiseb Formation. It contains rare and broadly spaced quartz veins (<1mm thick), and joints, close to KM12-02, 656300/7484635.

Mica-rich schist (MRS)

-Intensely foliated schist

This unit varies in colours ranging from medium grey-green, light green-green and reddish-brown. It is a very fine-grained, intensely foliated, less competent and more recessive compared to the QRS (Fig. 3.7). It consists predominately of muscovite, minor biotite and very minor quartz. Two sets of veins are evident within the unit; (1) veins cross cutting the foliation and (2) veins parallel to foliation.

Figure 3.7: Field photographs of the fine grained, intense foliated, less recessive mica-rich schist. Quartz veins parallel to foliation (> 1cm wide) are present at KM12-01, 657898/7484589.

-Speckled rarely foliated schist

The spotty/speckled schist has a medium grain size and consists of specks of mica and minor feldspars. It ranges from semi-massive to weakly foliated and forms part of the intensely foliated schist described in Figure 3.8. It only occurs in areas proximal to where the post-tectonic veins cross-cut the foliation and are observed to be as extensive as 3 m in length. No mineralisation was observed within the matrix of the speckled schist but oxidised sulphides and magnetite were observed from the veins.

Figure 3.8: Field photographs of the speckled schist associated with the quartz veins. Observed to be semi-massive to a weak foliation compared to the unaltered mica-schist at KM12-01, 657978/7484450.

Structural observations

Quartz veins range from 1cm to < 1m wide. Most the veins are gossanous with visible magnetite and hematite and cross-cut the foliation with minor non-gossanous veins parallel to the lithological foliation (Fig.3.8). A wall rock alteration product is observed in all places where the invasion of veins has occurred. Possible sulphide mineralisation along and within the margins of the veins, however it is not obvious as only ferruginous materials remain (Fig 3.9, Fig.3.10 and Fig. 3.11). Magnetite is observed on the quartz surfaces. The identified veins vary in thicknesses along strike and appear to swell towards the NNE and the gossanous nature of the veins varies along strike.

Although faults could not be identified from surface mapping, the locally rapid thickness changes noted within the schists and quartz veins strongly suggest the presence of normal faults. Many were however identified from the magnetic data available by the Kuiseb Copper Company (Fig. 3.4).

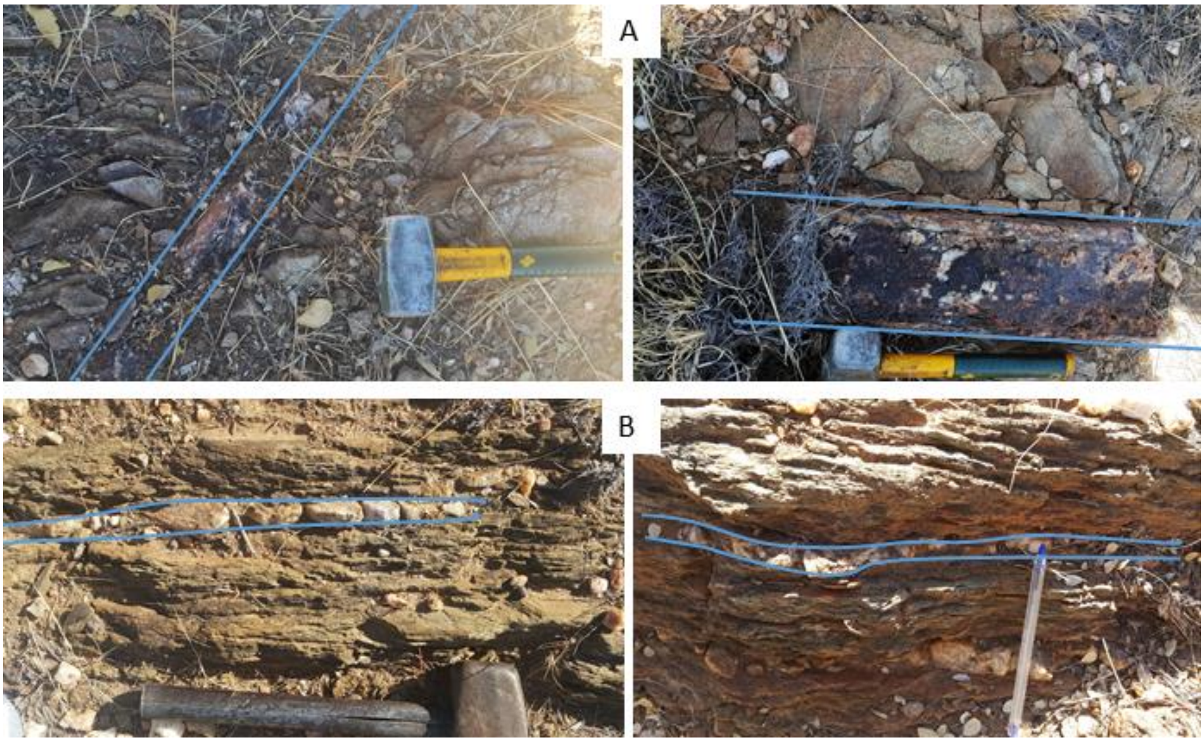

Figure 3.9: Field photographs of different quartz vein orientations within the Kariam Prospect. A: Gossanous quartz veins cross cutting the lithological foliation of the MRS leaving a speckled/spotty textured type of alteration everywhere they cut through around the vicinity of KM12-01 B: Quartz veins parallel to the lithological foliation of the MRS. Less ferruginous compared to the veins cross cutting the lithological foliation around the vicinity of KM12-02. The quartz veins are demarcated with the blue lines.

Figure 3.10: A-D: Field photographs showing different ferruginous quartz veins within the Kariam Prospect. Note that the ferruginous quartz veins cross-cut the lithological foliation and none are parallel to foliation at 657990, 7484463 near KM12-01.

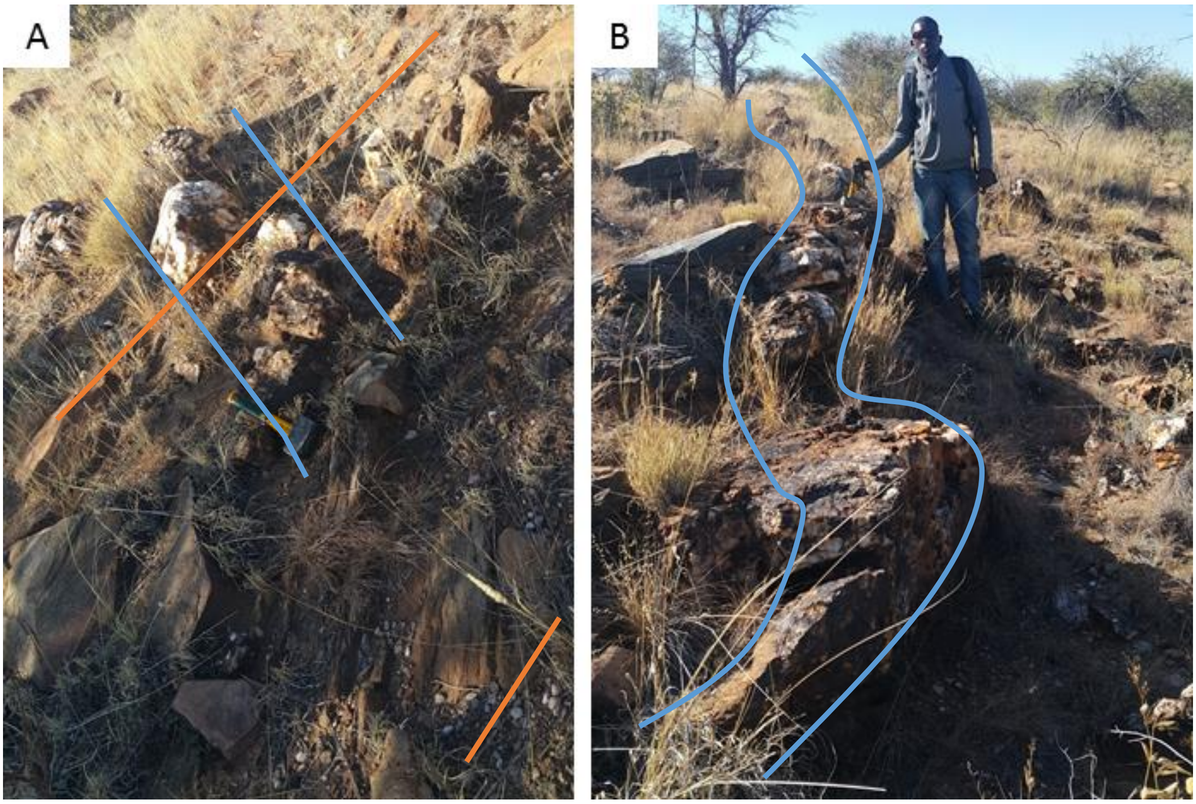

Figure 3.11: A-B) Field photographs showing extensive and thick gossanous quartz veins (marked in blue) cross-cutting the mica-rich schist. These veins only observed to cross-cut the highly-foliated mica rich schist (marked in orange) (657990, 7484430, close to KM12-01).

The structural measurements (foliation) derived from surface geology, suggest that the lithologies dip at 15° - 55° towards the south east between 220° - 320° (dip direction). Few direct contacts were observed in the field to support the obtained structural data. The measured structural data (Fig. 3.12C) are approximately similar to dip values of 20°-35° and a dip direction of 340° obtained by the Kuiseb Copper Company (2013) (Fig. 3.12B). Similarly, the orientations observed correspond with the NE-SW lithological strike orientations proposed by Shikongo and Hiveluah (2012) around the nearby Matchless Mine and the surroundings. The magnetite and hematite quartz-carbonate veins (strike of 20° - 45°) cross-cut the regional foliation while the non-gossanous veins are parallel to the regional foliation (220° - 320°) (Fig. 3.12).

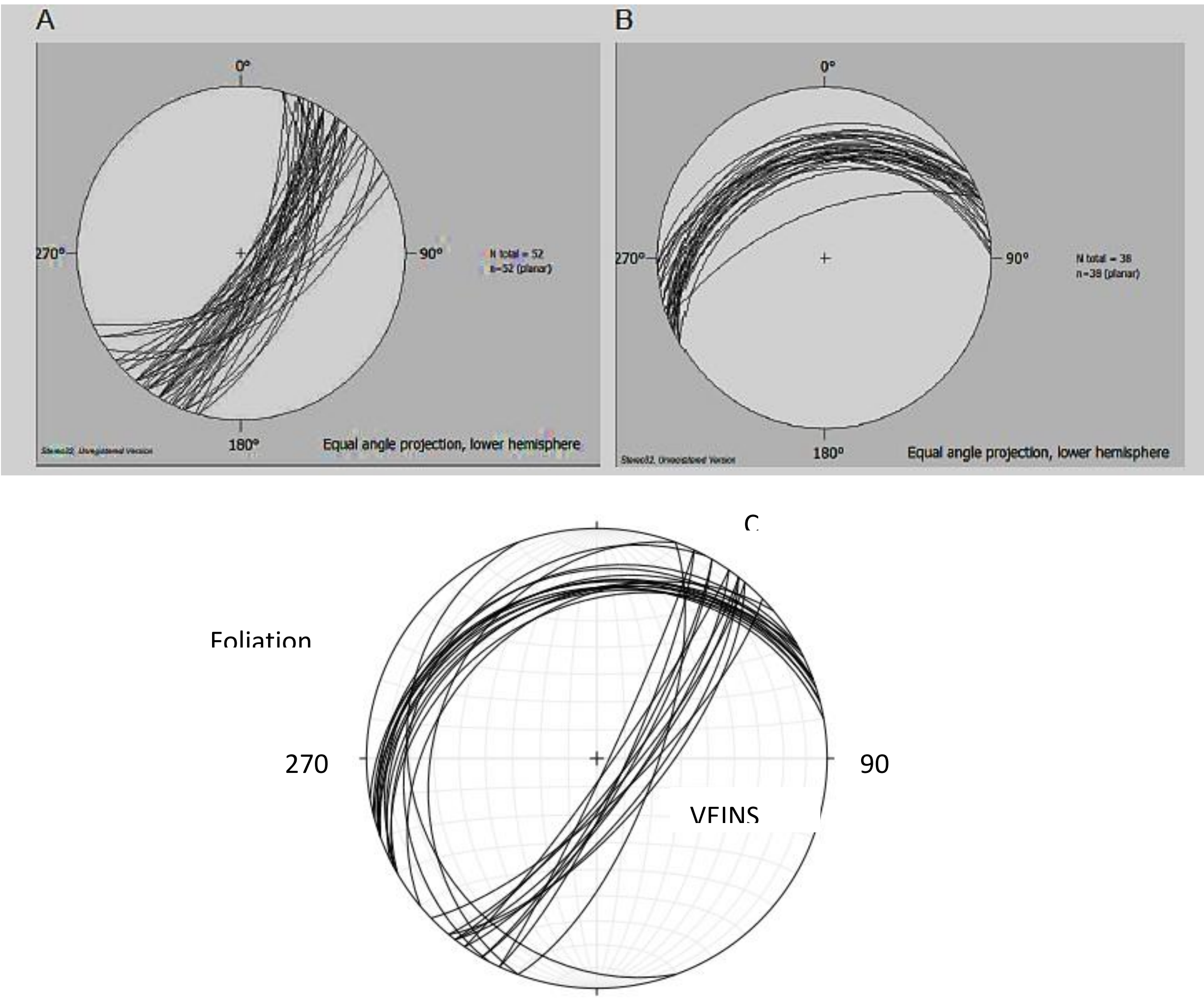

Figure 3.12: Plots of lithological foliation and veins within the Kariam Prospect. A) 52 Structural readings of the quartz-carbonate veins, B) 38 readings of the foliation of the schist. (Kuiseb Copper Company, 2013) and C: Plotted foliation and veins structural data from the study area. Limited data is due to poor exposure in the study area. SE dip direction was observed for the veins, with foliation readings between **220° - 320°.**

CHAPTER 4

BOREHOLE LOGGING

Detailed geological logging, which included lithological, structural, mineralisation and alteration was completed at the Geological Survey of Namibia (GSN) for the two existing boreholes; KM12-01 (EOH 399.15 m) and KM12-02, (EOH 302.45 m). A custom geological code dictionary was defined for the logging, see Appendix 2. Detailed log sheets for the two boreholes are found within Appendix 3 of this report. Sampling of the core was limited by the GSN and only 6 samples were collected for petrographic studies.

The Kuiseb Formation within the study area of the Kariam prospect consists of the schist package which varies between quartz dominated schist to mica dominated schist. The quartz dominated schist varies between light to medium grey in colour, commonly less foliated and more competent, while the mica-rich schist is dominated my muscovite, biotite, chlorite and sericite and has a well-defined mineral foliation. Through detailed logging the following mica-rich units were identified; muscovite schist, biotite chlorite schist (speckled unit), chlorite sericite schist while quartzitic schist also referred to as bleached halos and biotite schist were identified to belong to the quartz rich package.

The naming of these lithologies was based on the dominant minerals within each unit. Some of the names were however changed after petrographic examinations. Sampling of different lithologies was carried out randomly but was designed to include all rock units and few mineralised veins were observed. Detailed descriptions and photographs of each unit are presented below.

Table:3 Table with summaries of different rock units identified from core of the Kariam Prospect (See complete table in Appendix 4 with combined field, core and petrography observations).

Mineral packages	**Rock units**	**Brief descriptions (mineral composition, textures, ore minerals, structures, alterations)**
Quartz dominated	Quartzitic schist (bleached halo)	Dominated by quartz, medium grained and has a weak foliation, massive at certain spots. Consists of cross-cutting quartz-veins which host chalcopyrite, pyrrhotite, pyrite and molybdenite. Disseminated and patchy sulphides and oxides within the matrix proximal to the veins. It is an alteration product associated with the invasion of post-tectonic veins.
Mica dominated	Biotite schist	Consists of biotite and quartz, massive, rarely foliated. No sulphides observed. It is grey in colour and medium grained. Contains barren quartz-veins.

	Muscovite schist	Dominated by muscovite, highly fractured with an intermediate foliation, no mineralisation observed. Consists of barren quartz and carbonate veins.
	Biotite chlorite schist (speckled schist)	Consists of biotite, chlorite and quartz zoned clusters, local shearing, contain veins parallel to and cross cutting foliation. Disseminated pyrite within the matrix. Parts of this unit are affected by the massive chlorite alteration.
	Chlorite-sericite schist	Consists of chlorite and sericite, 90% of the veins are barren and the 10% are enriched with chalcopyrite and pyrrhotite. Intermediate foliation. Chlorite sericite alteration.

Muscovite schist (MS)

This generally forms part of the upper section of the boreholes making contacts with the speckled schist. It is grey-green in colour with additional colours which resulted from oxidation and weathering processes. The muscovite schist is fine grained and displays an intermediate foliation but intense fracturing (Fig. 4.1). It consists of mainly muscovite with minor amount of biotite and quartz. It contains barren quartz veins (1mm to 1cm wide) parallel to the mineral foliation and minor reddish carbonate veins (< 1cm wide) are observed. No fresh mineralisation identified within this unit besides the reddish spots which possibly resulted from the oxidation of sulphides.

Figure 4.1: Core photographs of the dry (A) and wet (B) highly fractured and foliated muscovite schist from the Kariam Prospect, borehole KM12-01 around 5.64m.

Biotite-chlorite schist (speckled schist) (BCS)

The speckled unit is light to medium grey lithology and it consists of quartz, biotite and chlorite. The biotite and chlorite occur as clusters within the fine-grained matrix defining a speckled texture (Fig 4.2A and B). It is commonly less foliated but foliation is well defined were local shearing is experienced (Fig 4.2A). Additionally, it is a competent unit more receptive to alteration and less receptive to fracturing than the MS previously described. This unit serves as a host rock to two sets of quartz-carbonate veins; i) quartz veins (1mm to 1cm wide) parallel to the foliation and ii) quartz - carbonate veins (>0.5cm to >1m wide) which cross-cut the foliation at a high angle.

Figure 4.2: Core photographs showing the speckled schist (biotite chlorite schist) from KM12-01 at depth 42.8 m-43.8m. A) Typical local shearing associated with biotite-chlorite and sericite alteration. B) Speckled nature of the biotite chlorite schist with a boudinaged quartz vein.

Chlorite-sericite schist (CSS)

The chlorite sericite schist is a medium green-grey with a strikingly dull green colour, fine-grained unit. It consists of chlorite, sericite, biotite and quartz. The mineral foliation is well preserved and has quartz veins (<1cm to 30cm wide) which are parallel to and cross cut the foliation (Fig. 4.3A & B). Moreover, some of the quartz veins are folded and display asymmetric type of folds (Fig. 4.3B). However, despite the wide range of available veins more than 90% of these veins are barren and only 10% contain sulphides, mainly chalcopyrite and pyrrhotite.

Figure 4.3: Representative core photographs of the chlorite sericite schist. A) From borehole KM12-01 at 133- 134 m, it shows a green-grey schist with quartz veins parallel to foliation in range of >1 mm to 30 cm wide. B) Chlorite sericite schist with folded mineralised (chalcopyrite and pyrrhotite) quartz veins developed within the foliation (KM12-02 at 238.3 m).

Biotite schist

The biotite schist is dark grey in colour, fine grained and massive. It contains little or no foliation, no fractures and it is rarely veined. It generally consists of black platy biotite minerals and white feldspars which are possibly albite in composition. There are no sulphides or other minerals present within the matrix or within the quartz veins of this unit.

Figure 4.4: Core photographs of the biotite schist, from KM12-01 at 115.1 m-116 m. It is a massive unit with little or no foliation, rarely veined and contains no sulphides.

Quartzitic schist/bleached halo

This unit occurs in between the biotite chlorite schist described earlier. The colours range from light cream to light grey. It was however not logged as a separate unit from the biotite chlorite schist. It generally consists of a quartz-rich matrix. The stand out features within the unit are the quartz-carbonate veins that cross-cut the foliation with majority of these veins enriched with sulphides (Fig. 4.5A). The veins contain disseminated magnetite and pyrite within the matrix (Fig. 4.5B).

Figure 4.5: Core photographs of the quartzitic schist. A) Quartz-carbonate veins cross cut the foliation of a medium grey quartzitic schist, KM12-01 at 110 m -111 m. B) Cream bleached schist which contains cross-cutting chalcopyrite and pyrite-rich quartz-carbonate vein and disseminated magnetite within the matrix, from KM12-01 at 397.3 m.

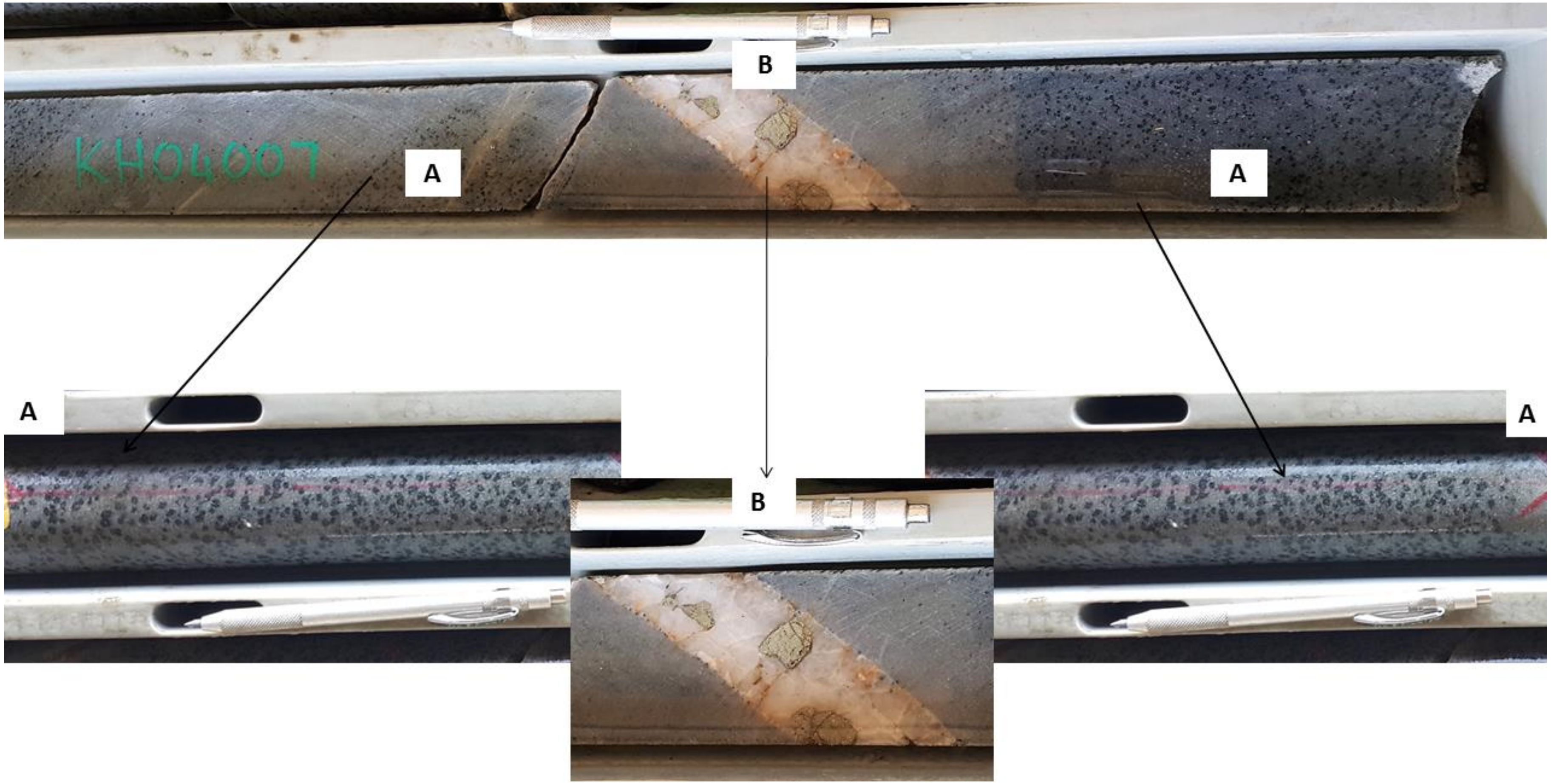

Figure 4.6: Core photographs showing contacts between A) speckled (biotite chlorite) schist and B) quartzitic (bleached) schist in relation to the post tectonic quartz-carbonate veins forming the footwall and hanging wall of the vein from KM12-01 at 33.22 m- 34.25 m.

The bleached, quartzitic schist (Fig. 4.6B) occurs in between the biotite chlorite (speckled) schist (Fig 4.6A), which making up the hanging wall and footwall of the quartz-carbonate veins. Within the bleached-quartzitic schist are quartz-carbonate veins which cross cut the lithological foliation (Fig 4.6B and 4.9A-E) and this bleached unit is observed to be approximately 4 to 5 times the width of the vein. It is believed to be an alteration product caused by the invasion of the quartz-carbonate veins within the biotite chlorite schist.

Alteration

Different alteration features were identified in the core, namely speckled biotite and chlorite alteration, bleached halo (quartzitic) alteration and chlorite and sericite alteration. The biotite and chlorite speckled alteration is defined by clusters of biotite and chlorite within a fine-grained matrix (Fig4.7A). From field work, this alteration is linked to the post tectonic veins. The speckled/spotty alteration is continuous and alteration zones can be as thick as 60 m.

The chlorite sericite alteration displays a dull green-grey colour within the matrix of the host rock (Fig. 4.7B). It is within the foliation and matrix of the host unit. Sericite alteration is also noted within the biotite chlorite (speckled schist) associated with local shearing within the unit (Fig. 4.7B). Most importantly, the chlorite sericite alteration is associated with quartz veins which are enriched with minor sulphides.

The bleaching/quartzitic alteration is massively distributed and makes up the matrix. It is attributed to the invasion of post tectonic quartz-carbonate veins which cross cut the foliation (Fig. 4.6C & C'). The bleached halos are measured to be approximately 4 to 6 times the width of the veins. Interestingly, the majority (>80%) of the quartz-carbonate veins associated with these halos are hosts to sulphide mineralisation.

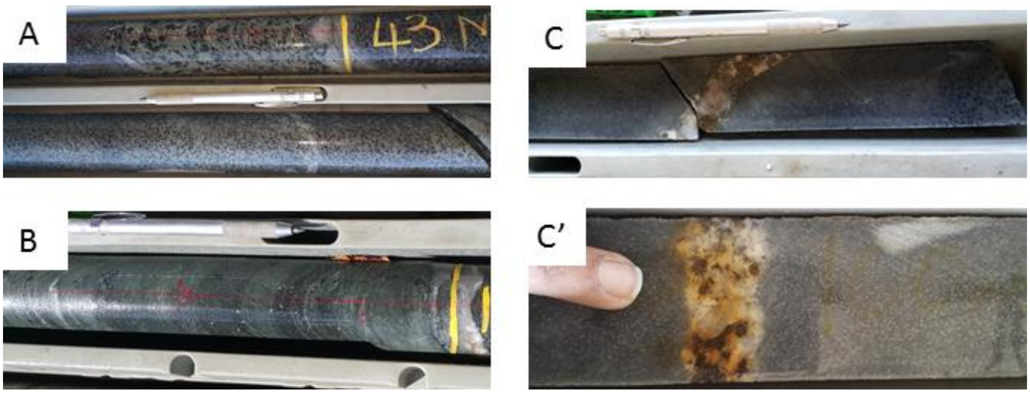

Figure 4.7: Core photographs showing different alterations identified . A) Biotite chlorite speckled alteration and local shearing with minor sericite alteration (KM12-01 at 43m). B) Chlorite-sericite alteration along the foliation of the host unit, KM12-02 at 144 m. C and C') Bleached halos with quartz-carbonate veins which cross cut the lithological foliation at a high angle, KM12-01 (209 m. The veins are enriched with sulphide mineralisation mainly pyrrhotite and minor chalcopyrite (KM12-01 at 72.4m and 100m respectively).

Distribution of the ore minerals

The Matchless Belt is a home to base metal mineralisation and it is with no doubt that the following sulphides and oxides were identified from the Kariam Prospect. The main oxide within the prospect is magnetite and trace hematite, and the common sulphides are pyrrhotite, chalcopyrite, pyrite and molybdenite in variable amounts. The majority of these sulphides are in quartz-carbonate veins hosted by quartzitic-bleached schist with minor sulphides hosted by the chlorite sericite schist of the Kuiseb Formation. The dominant sulphide is pyrrhotite and the dominant oxide identified is magnetite. Fine-grained disseminated mineralisation is locally observed and associated with the matrix of host units (Fig. 4.8A-D). Moreover, mineralisation occurs as patches, blebs and veinlet stringers within the quartz-carbonate veins and areas proximal to these veins.

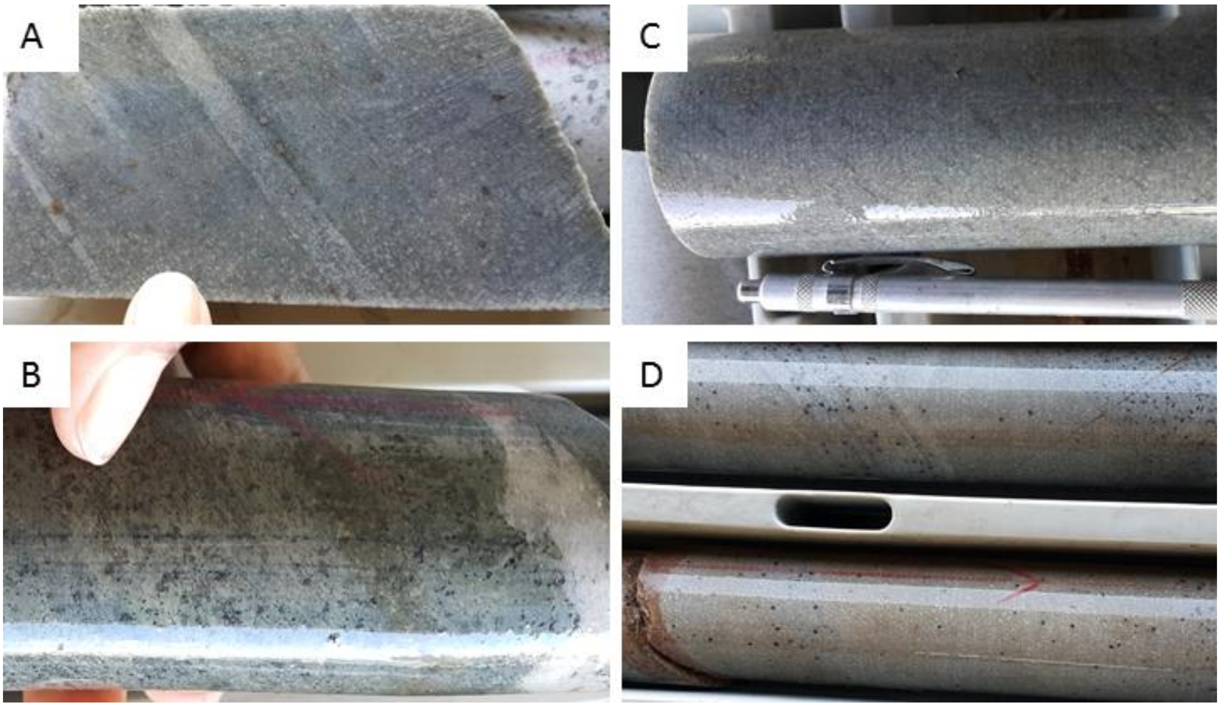

Figure 4.8: Core photographs showing the distribution of sulphides and oxides within the matrix of the host rocks from. A) Disseminated magnetite within the matrix of the bleached/quartzitic schist, KM12-01 at 62.5 m. B) Very small stringer of chalcopyrite within a sheared speckled biotite chlorite schist, KM12-01 at 72.8 m. C) Pyrrhotite in veinlet form parallel to each other in the fine-grained matrix of the bleached/quartzitic schist (KM12-01, 172.2 m) and D) Disseminated magnetite and pyrite in the bleached halo, KM12-01 at 109.2 m.

The main hosts of sulphide mineralisation within the Kariam Prospect are the quartz-carbonate veins which cross-cut the lithological foliation, hosted mainly by quartzitic-bleached schist with minor hosted by chlorite sericite schist. Mineralisation is discontinuous within these veins which are between <0.5 cm to over 1 m wide. Sulphides occur as patches, blebs, disseminated and they fill fractures in-between the veins (Fig. 4.9A-E and Fig. 4.10A-D). Pyrite and chalcopyrite are observed as rims within the pyrrhotite grain (Fig. 4.9A, B and D). Important to note is that not all cross-cutting veins are mineralised.

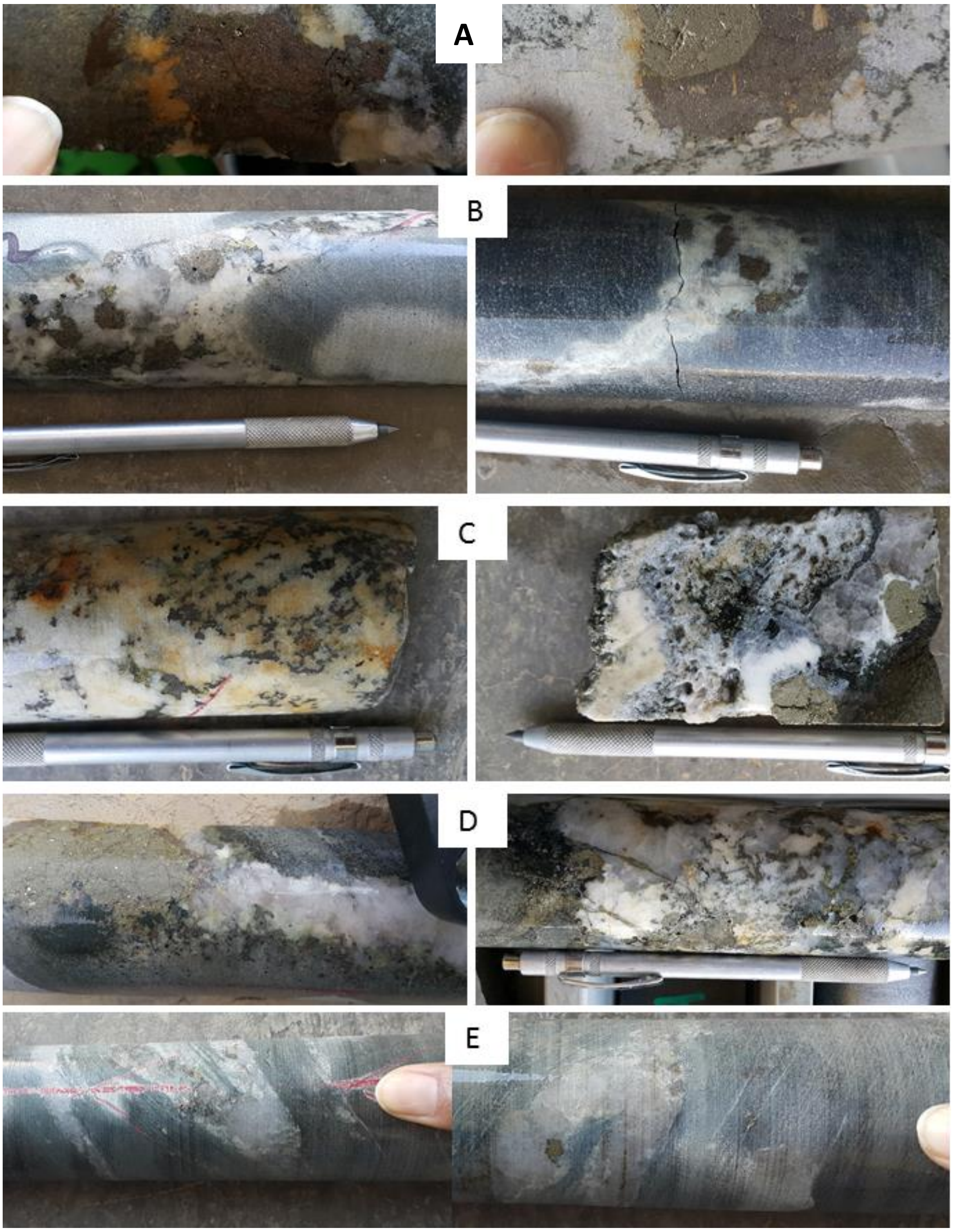

Figure 4.9: Core photographs showing quartz-carbonate veins and the sulphides hosted within them. A) Patches of pyrrhotite, chalcopyrite and pyrite within a quartz-carbonate vein. Pyrite and chalcopyrite form rims within the chalcopyrite grain (KM12-01). B) Patches of pyrrhotite and chalcopyrite within a quartz-carbonate vein (KM12-01). C) Disseminated pyrrhotite and pyrite patches in a carbonate dominated vein (KM12-01 at 112.6 m-113 m). D) Patches of pyrrhotite, pyrite and minor chalcopyrite within quartz-carbonate veins and within fractures between veins. E) Folded quartz veins within a chlorite sericite schist with minor patches/blebs of pyrrhotite and chalcopyrite (KM12-02 at 238.8 m).

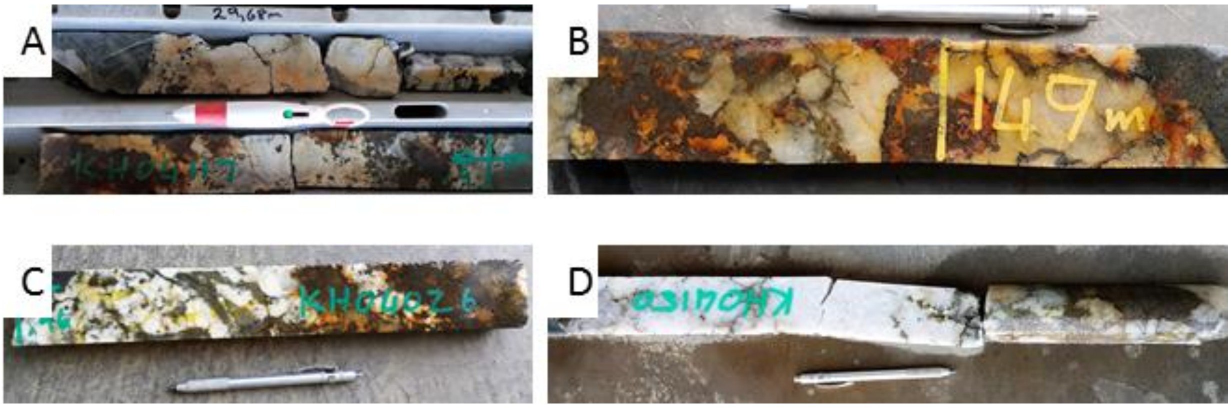

Figure 4.10: Core photographs showing the thicknesses of some quartz-carbonate veins and the mineralisation they host. A and C) Milky quartz-carbonate veins in between bleached schist hosting ferruginous sulphides, mainly pyrrhotite and chalcopyrite and minor pyrite (KM12-01 at 29.68 m and 63.96 m- 64.58 m respectively). B and D) Gossanous quartz veins hosting sulphides with pyrrhotite being dominant and chalcopyrite. The sulphides fill fractures within the veins (KM12-01 at 149 m and KM12-02 at 127.1 m -127.70 m respectively).

Sulphide mineralisation at the Kariam prospect is dominated, but not limited to the post-tectonic quartz-carbonate veins which cross cut the lithological foliation (Fig. 4.9 and 4.10), it is also disseminated within the matrix of the host rocks proximal to these veins (Fig. 4.8). The Matchless deposits are characterised by the abundance of pyrite and pyrrhotite with associated chalcopyrite and trace amounts of cubanite and molybdenite (Klemd et al., 1987), and they are known to be semi-massive, massive and banded (Killick, 2000) unlike the Kariam mineralisation which is vein-hosted.

At Onganja, a deposit close to the Matchless Belt, the zones of mineralisation are restricted to elongated domal structures with a broad stratigraphy consisting of basal quartz-plagioclase-biotite schist followed by epidote-quartz rocks and amphibolite schist with most of the mineralised veins concentrated in the immediate footwall of the epidote-quartz unit (Moore, 2010). Moreover, the quartz-plagioclase biotite schists have been variably altered in contact with the mineralised veins (Moore, 2010), and this is similar to what has been observed within the biotite chlorite schists in contact with the veins of the Kariam Prospect. These two deposits are all hosted by the quartz-carbonate veins but the host rocks are different.

Observed Structures

Structures believed to have formed during the early deformation episodes are recognised as schistose fabrics and quartz veining (generally on a cm scale which are parallel to the foliation) (Fig 4.11A-E). Additionally, the folded quartz veins within the biotite chlorite schist and bleached schist (Fig 4.11A, B and E) might have possibly also formed during the early deformation with a late deformation episode resulting in quartz-carbonate veins cross cutting the lithological veins (Fig. 4.11F).

The main structural control for mineralisation in the Kariam Prospect are the quartz-carbonate veins which cross-cut the foliation (Fig. 4.11F) and no mineralisation was observed in veins parallel to foliation (4.11C and D). Crenulation folding which probably represents the deformation episode 3 in the Southern Zone was observed and no mineralisation associated with it (Fig. 4.11A). Local shearing of the biotite chlorite (speckled) schist was also observed (Fig. 4.11D).

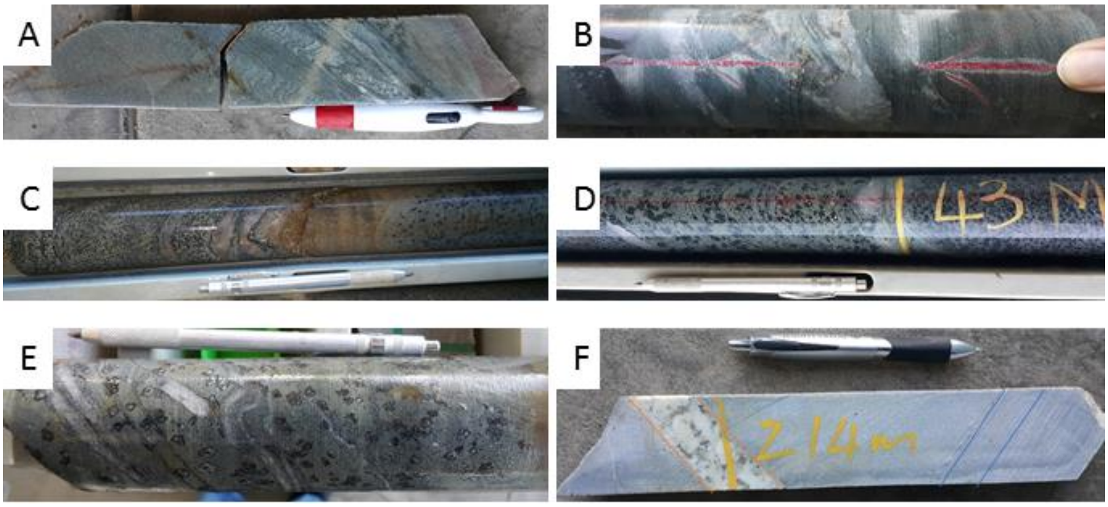

Figure 4.11: Core photographs showing structural features identified in the Kariam Prospect drill core. A) Crenulation folding within a bleached-quartzitic schist. B) Folded quartz vein within a chlorite-sericite schist. It contains minor specks of chalcopyrite and pyrrhotite, KM12-01 at 238.8m. C) Quartz veins on a scale of cm, parallel to the foliation of the speckled biotite chlorite schist. D) Local shearing of the porphyroblasts rich schist, KM12-01 at 42.8 m - 43.2 m. E) Folded quartz veins within the speckled biotite chlorite schist, no mineralisation associated with these veins (KM12-02, 70.2 m) F) A veined and foliated bleached-quartzitic schist. The quartz-carbonate is demarcated with the orange lines and the foliation it cross cut is indicated with the blue lines. The vein is enriched in sulphides (chalcopyrite and pyrrhotite with minor molybdenite) from KM12-01 at 214 m.

Borehole stratigraphy

Two stratigraphic columns were produced from logging the boreholes KM12-01 and KM12-02 (Fig. 4.12). Detailed descriptions of identified units are provided at the beginning of this section and the localities of both boreholes are provided in Figure 3.1. Both boreholes consist of the Kuiseb Formation schist succession and the logged lithologies are as follows, biotite chlorite schist, chlorite sericite schist, muscovite schist and the undifferentiated unit that is made up of two or more closely intercalated and altered units.

NB: the bleached halos (quartzitic schist) were logged as part of the biotite chlorite schist due to their thin widths in places.

The muscovite schist makes up the top layer of the boreholes and extends as deep as 20 m. The dominant lithology in KM12-01 is the speckled biotite chlorite schist mainly intercalated with the biotite schist and in KM12-02 the main lithologies are the speckled biotite chlorite schist and the biotite schist (Fig 4.12). The BCS can be extensive as 40m wide so as the biotite schist.

Pyrite and magnetite mineralisation was intersected in KM12-01 at depth between 23-26 m. Magnetite is disseminated within the matrix of the bleached halos, while pyrite occur as blebs and patches within matrix and in veins, cubic pyrite grains do occur. The very first chalcopyrite bleb was observed at around 41 m in a milky quartz vein together with pyrite. Pyrrhotite, the dominant sulphide was first intersected at depth of 57 m associated with chalcopyrite and pyrite grains in a quartz vein. The other sulphide identified in borehole KM12-01 is molybdenite, occurring in trace amount and observed within a quartz-carbonate vein between 63.9-64.5 m together with chalcopyrite, pyrite and pyrrhotite. Over 80% of the bleached units have veins which host the sulphides. Good sulphide grades (> 2% of po+ cp, estimation from core) are associated with gossanous veins which can be extensive as 1 m. Within the chlorite sericite schist, the first sulphide observations were made at around 135 m with pyrrhotite and chalcopyrite occurring as blebs within the quartz vein. Sulphide mineralisation drops towards end of hole, see complete log in Appendix 3.

In borehole KM12-02, mineralisation namely pyrite, pyrrhotite and chalcopyrite were intersected at 29.6-30.9 m within a 1.2 m wide quartz-carbonate vein. Sulphides have textures like those observed in borehole KM12-01. Molybdenite on the other hand was observed as tiny blebs at around 68.73-70.57 m together with pyrite, chalcopyrite and pyrrhotite. Mineralisation was minimally observed in this borehole compared to KM12-01. The host units and structural controls are similar in both boreholes. There is also a decrease in sulphide mineralisation towards end of hole, see complete log in Appendix 3.

From the available geochemical data obtained from AAS the following copper values were obtained. High copper grades of ± 0.1 % were encountered in borehole KM12-01 at the following interval; 63.96m - 64.58 m, 148.65 m - 149.15 m, 175.4 m - 175.7 m, 195.10 m - 195.10 m, 321.15 m - 321.5 m, 336.2 m-337.25 m and 354.6 m – 355 m, and the following intervals from KM12-02 have copper values greater than 0.1%; 29.50 m – 30.90 m, 45.7 m – 46.10 m, 57.1 m – 57.80 m, 76.20 m – 76.80 m, 77.1 m - 77.4 m, 127.10 m – 127. 7 m and 149.45 m – 149.74 m.

The bleached-quartzitic halos host the quartz-carbonate veins with the high copper values mentioned above, with an exception at the interval 149.45 m -149.74 m in KM12-02, where the high values are in veins associated with the chlorite-sericite schist (Fig. 4.12). Minor gold values were detected from the core samples submitted for AAS and ICP analyses by Kuiseb Copper Company. The dominant sulphide is pyrrhotite with subordinate chalcopyrite, minor pyrite and trace molybdenite. Mineralisation is dominant but not restricted to post-tectonic veins, it is also associated with areas proximal to these veins. Due to limited borehole data and the distance between KM12-01 and KM12-02 (>3 km apart), correlations between the two boreholes could not be made.

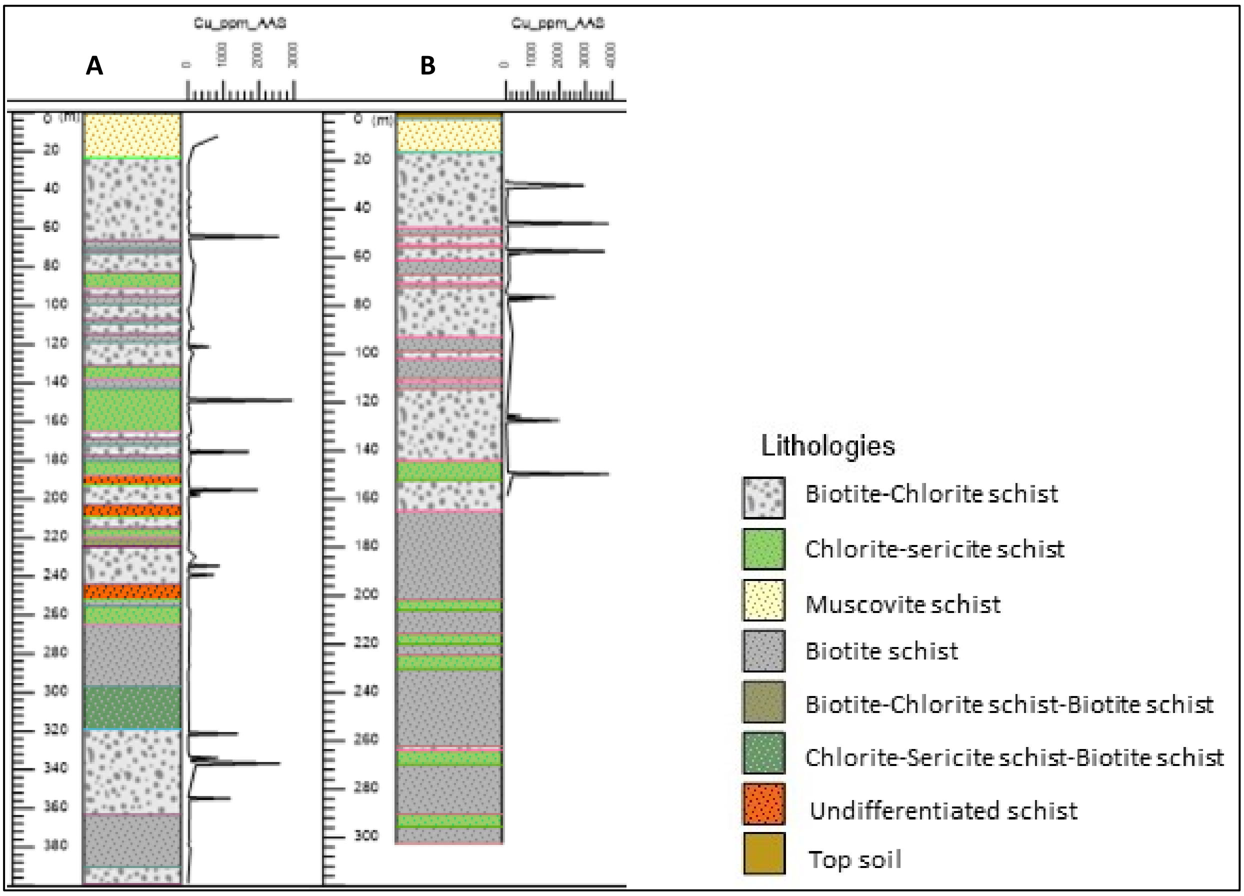

Figure 4.12: Stratigraphic columns produced from logging boreholes KM12-01 (A) and KM12-02 (B) respectively. The borehole lithologies are made up of altered Kuiseb Formation schist successions. The copper values in parts per million (ppm) are represented by the blacklined log opposite each column. Continuous lines are used at intervals with no available Cu values.

CHAPTER 5
PETROLOGY

This chapter outlines observations made during petrological examination of representative samples of the different rock types identified during field mapping and borehole logging. Therefore, the main aims are to be able to identify different rock types, obtain a better understanding of the mineralogy, textural relationships, approximate mineral percentages present and structural features of the different rock types. A total of 12 thin sections and 8 polished sections were used and the detailed field observations samples used for petrography are described in Chapter 4.

In the field two different rock types were identified and during core logging four different rock types were identified. The characteristics of these lithologies and correlations are presented in Table 4. Variations in composition and texture visible in hand samples were used as basis for sample collection. Based on preliminary hand specimen observations, the schists consist of varying amount of quartz, muscovite/sericite, biotite, chlorite, feldspar and sulphides, while carbonate minerals were only identified from thin sections. Broadly speaking, the mineralogy of the quartz-rich schist and the mica-rich schist are relatively simple. Detailed descriptions on the mineralogy of each rock unit can be found in Appendix 4.

Table 4: Table showing characteristics of lithologies and the correlations of different rock types within the Kariam Prospect.

	Field name	**Core name**	**Thin-section name**	**Brief Description**
Mica-rich schist	Muscovite schist		**Muscovite schist**	It is composed of muscovite (60%), chlorite (25%) and biotite (15%). There are two sets of foliations; i) continuous alignment of muscovite and ii) biotite foliation sub-parallel to the muscovite foliation (Fig. 4.1). It is very fine grained and intensely foliated. Associated with two sets of quartz veins. Minor pyrite within the matrix.
		Chlorite-sericite schist	**Chlorite-Sericite Schist**	Consists of chlorite (20%), biotite (10%), sericite (40%), quartz (30%) and carbonate minerals (<1%).Continuous foliation displayed by fine grained mica (blue) and another set of later foliation defined by acicular biotite overgrowing

				the early foliation (orange).
	Speckled schist	Biotite-chlorite schist	**Biotite-chlorite schist**	Consists of zoned clusters of quartz (10%), biotite (15%) and chlorite (20%) within the fine-grained matrix made up of sericite/muscovite (50%). It has spotty texture and veined. Local shearing and folding of clusters are observed.
Quartz-rich schist		Bleached schist	**Quartz-carbonate schist**	Consists of quartz (60%) and vuggy carbonate (30%) and feldspar and muscovite (10%). Foliation displayed by irregular and elliptical quartz grains, with a weak continuous foliation displayed by muscovite aligned parallel to each other. Host to magnetite, pyrite and minor chalcopyrite. Major host of sulphide rich quartz-carbonate veins.
	Quartz-mica schist	Quartz schist	**Quartz-muscovite schist**	Dominant minerals include quartz 60% and muscovite (40%). Continuous foliation displayed by muscovite and quartz grains aligned parallel to each other.

Mica-rich schist

Muscovite-rich schist

This lithology consists of muscovite, chlorite and biotite (Fig 5.1). The dominant mineral muscovite makes up 60% of the rock sample, 25% chlorite and 15% biotite.

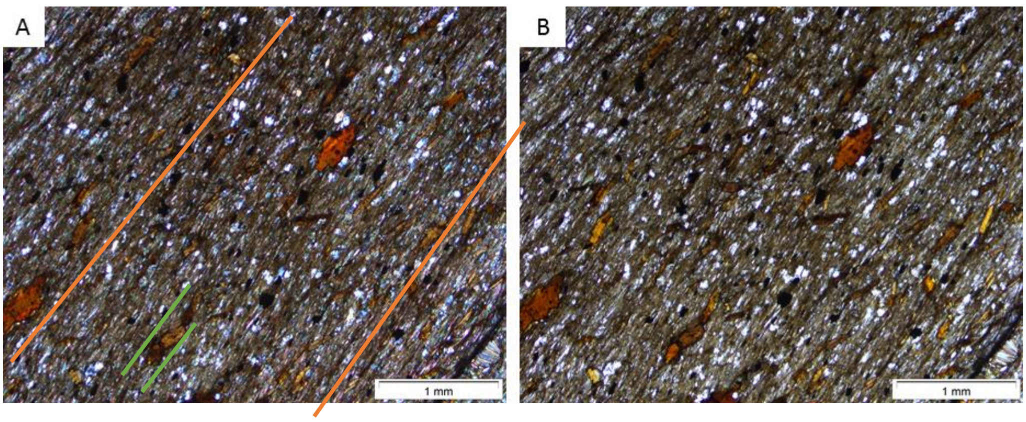

Figure 5.1: Thin section microphotographs of the field sample of the muscovite-rich schist within the Kariam Prospect in A: cross polarised light (XPL) and B: plane polarised light (PPL) respectively.

This unit consists of predominately muscovite with biotite sub-parallel to the muscovite fine-grained foliation, close to KM12-02 at E: 656350, N: 7484970.

Two sets of foliations are observed within this lithology; i) continuous foliation defined by fine-grained muscovite grains and ii) discontinuous foliation sub-parallel to the muscovite defined by the acicular biotite grains, there is an overgrowth of biotite over the muscovite (Fig. 5.1).

-Biotite-Chlorite Schist

This rock unit consists of chlorite, sericite, feldspar, biotite and minor carbonate. The dominant mineral sericite makes up 50% ground mass, chlorite and biotite makes up 20 % and 15 % respectively, 10 % quartz and <5 % carbonates. The sericite makes up the rocks ground mass while feldspar, biotite and chlorite are zoned and display a speckled texture within the finer matrix (Fig. 5.2A). Individual euhedral biotite and chlorite grains are disseminated throughout the fine-grained matrix. The carbonate mineral appears vuggy, displays no cleavage, forms little aggregates and has a low birefringence (Appendix 1). Additionally, the carbonate mineral engulfs the micas (Appendix 1 Fig 9.3 and 9.4). Local shearing and folding of the clustered mica has occurred (Fig. 5.2B).

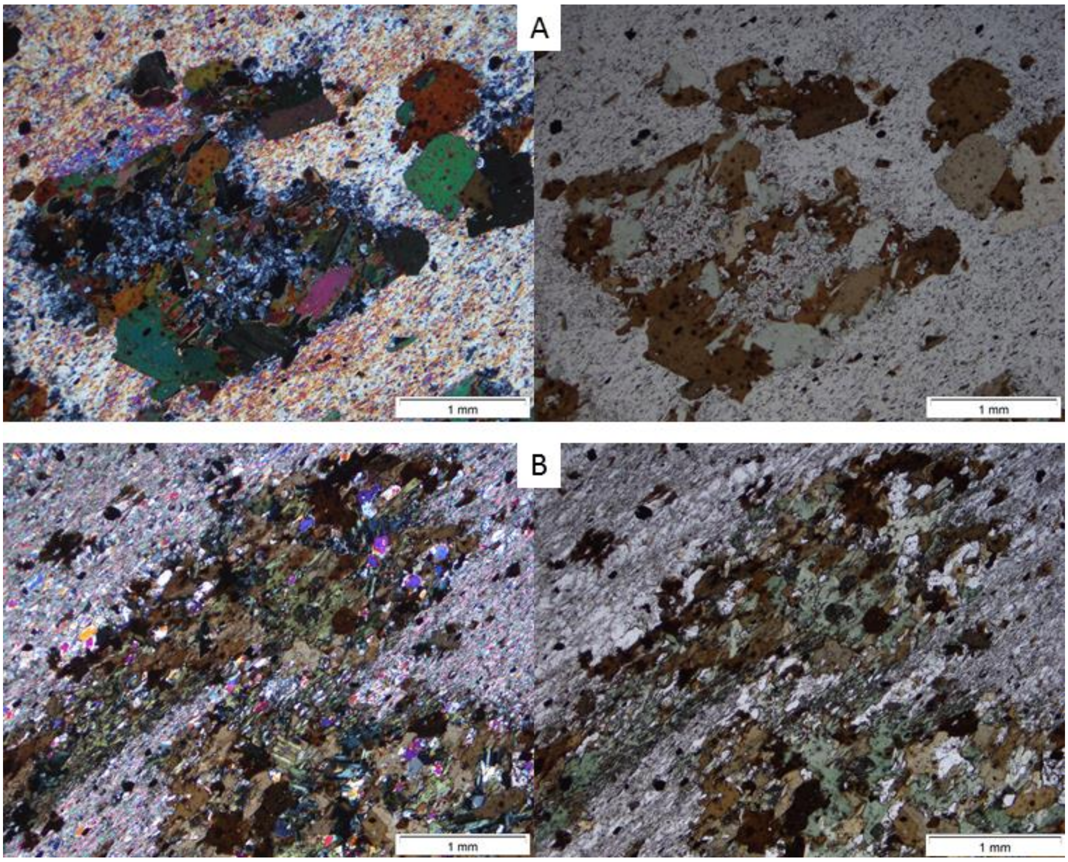

Figure 5.2: Thin section microphotographs in XPL (left) and PPL (right) of the biotite chlorite schist. A) Zoned biotite, chlorite with quartz making up the core. The ground mass is made up of fine-grained sericite/muscovite which displaying a crenulation cleavage, KM12-01 at 165 m. B: Folded clusters of biotite-chlorite within a fine-grained sericite/muscovite matrix, KM12-01 at 73 m.

The sericite displays a dominant fine-grained continuous foliation (crenulation cleavage). The zoned grains of feldspars, biotite and chlorite are affected by local shearing, thus displayed as elongated grains (Fig 5.2B). There is an overlap in the growth of biotite and chlorite displayed by a very sharp junction between these two micas.

-Chlorite Sericite Schist

The dominant minerals within this lithology include quartz, sericite/muscovite, chlorite, biotite and trace carbonate. The quartz grains are euhedral and interlocked with each other whereas chlorite and biotite grains are acicular (Fig 5.3A and B). The quartz grains display undulose extinction and the chlorite grains show a blue anomalous extinction colour. Quartz boudins are present but not common. There is an overgrowth of biotite and chlorite. The vuggy carbonate forms little aggregates which engulf the mica and the quartz grains.

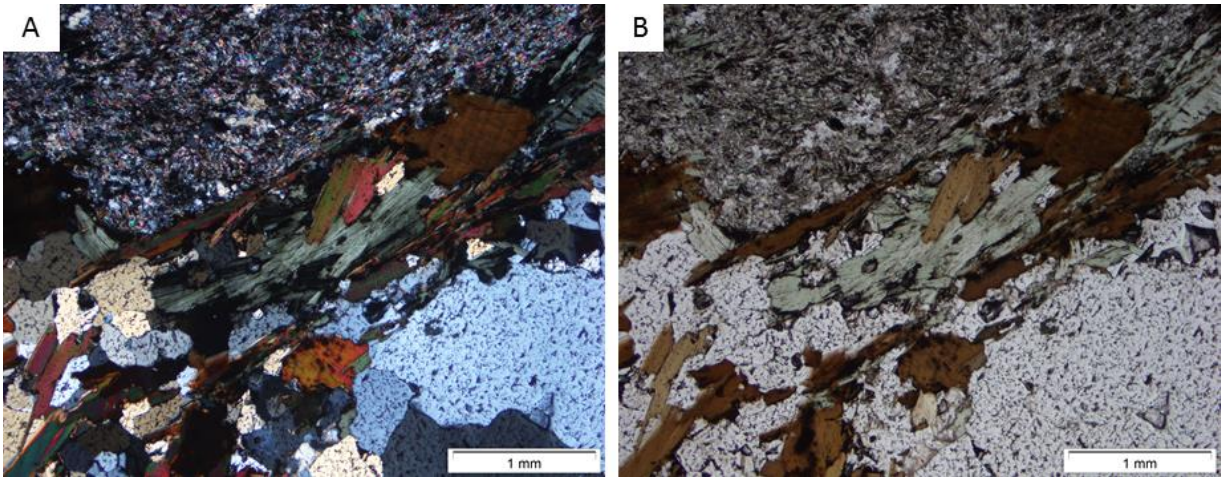

Figure 5.3: Thin section microphotographs of the chlorite-sericite schist in XPL (left) and PPL (right) fromKM12-01 at 99.4 m. A) The dominant minerals include sericite, quartz, chlorite and biotite. Folded layer of fine grained muscovite/sericite in quartz. Note the difference in grain size of recrystallized quartz (coarse), medium grained quartz and sericite (fine). Quartz boudins are present but not common.

Two different quartz-forming events are observed: i) medium-grained quartz associated with the fine-grained sericite and ii) coarse-grained post tectonic quartz veins. Regular quartz grain boundaries are also present. A clear contact/boundary between the medium grained quartz and the granoblastic quartz is observed. There is recrystallisation in the microfold hinges of the mica (crenulated schistose fabric defined by the orientation of the muscovite crystal). A continuous fine-grained foliation formed by the alignment of mica around the quartz is observed. Some of the quartz veins are folded, a feature visible from hand specimen as well.

Quartz-rich schist

-Quartz-muscovite schist

This lithology generally consists of quartz, muscovite mica, minor biotite and trace carbonate. Quartz is a major mineral in most of the rock samples examined and it makes up approximately 50 % of the rock unit. It displays a mosaic texture of equigranular quartz grains (Fig 5.4) which display undulose extinction. Acicular muscovite and biotite make up about 40% and 10 % of the rock respectively.

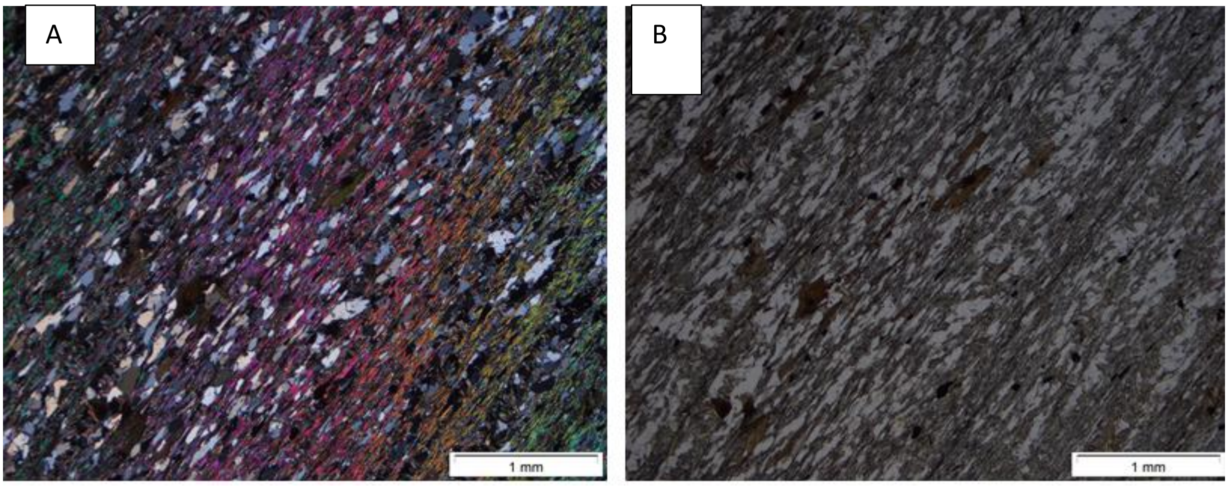

Figure 5.4: Thin section microphotographs for the quartz-mica schist from a field sample in XPL (A) and PPL (B). Dominant minerals include quartz and muscovite with minor biotite, from KM12-01 vicinity.

A continuous anastomosing foliation is defined by the mica (muscovite and biotite) which is also defined by the coarse-grained elongated quartz. The quartz-muscovite schist displays a continuous parallel foliation resulting from the alignment of muscovite. The quartz occurs as rounded, elliptical and irregular forms also elongated sub-parallel to the foliation. Pyrite is the only sulphide observed within the matrix of the unit and it occurs as patches and disseminations.

-Quartz Carbonate Schist

This rock unit generally consists of quartz, carbonate, minor muscovite and feldspar (albite) and trace biotite. Quartz and feldspars grains are interlocked with each other. An undulose extinction is displayed by the quartz grains and the feldspar grains have lamellae twins (Appendix 1, Fig. 9.1 and 9.2). The carbonate grains have a vuggy texture and they engulf the quartz and feldspar grains giving the poikiloblastic texture (Fig. 5.5)

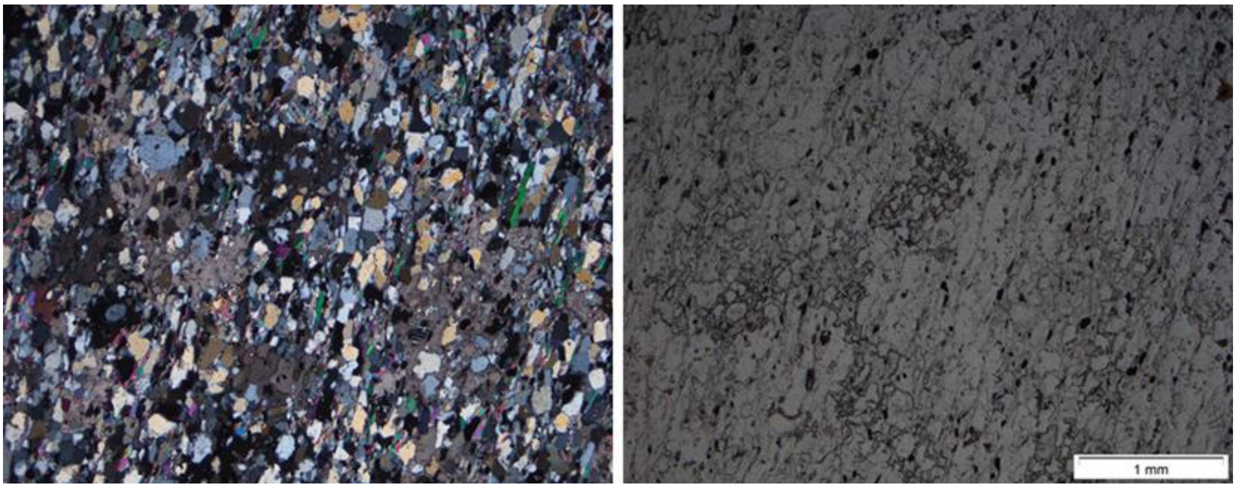

Figure 5.5: Thin section microphotographs of the quartz-carbonate schist in XPL (left) and PPL (right). Dominant minerals include quartz and carbonate with muscovite in minimal amount. Weak foliation is displayed by the coarse-grained quartz grains and the muscovite, KM12-01 at 109.78 m.

The main foliation arises from the mica, mainly muscovite aligned parallel which is also defined by a coarse grained continuous foliation displayed by the quartz orientation (Fig 5.5). Clear sharp contact occurs between the quartz-carbonate schist (bleached halo) and the biotite chlorite schist (speckled unit).

Quartz-carbonate veins

The quartz-carbonate veins are the major hosts of the sulphides within the Kariam Prospect. They are observed to be in contact with the host rocks, mainly the quartz-carbonate schist (bleached schist) (Fig. 5.6). The veins were observed to contain a great amount of carbonate minerals than what is observed within the handspecimen.

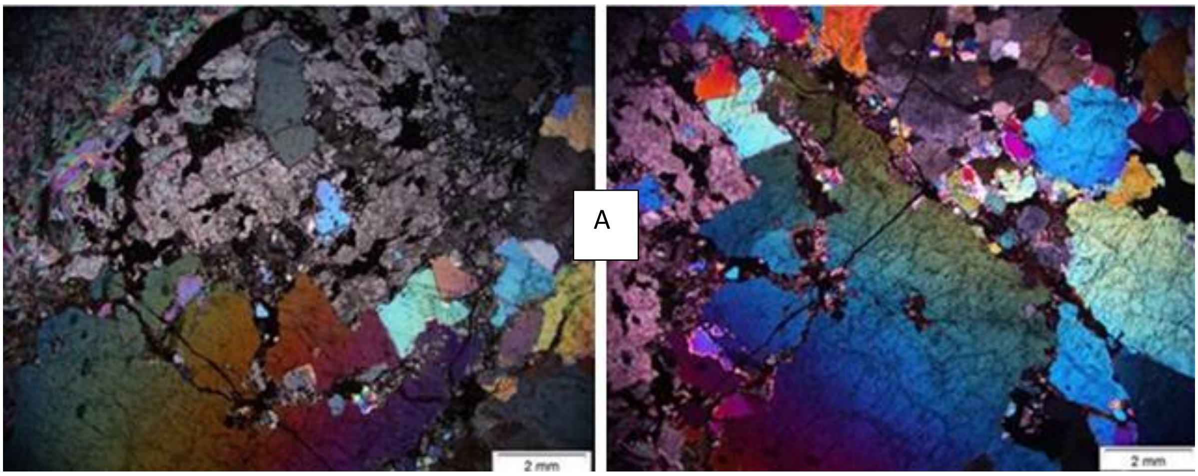

Figure 5.6: Thin section microphotographs of the quartz-carbonate veins, KMM12-01 at 108.5 m. Consists of quartz, carbonate, mica (host rock) and sulphides. The sulphides fill fracture and occur as patches and disseminated within the host rock in areas proximal to the veins.

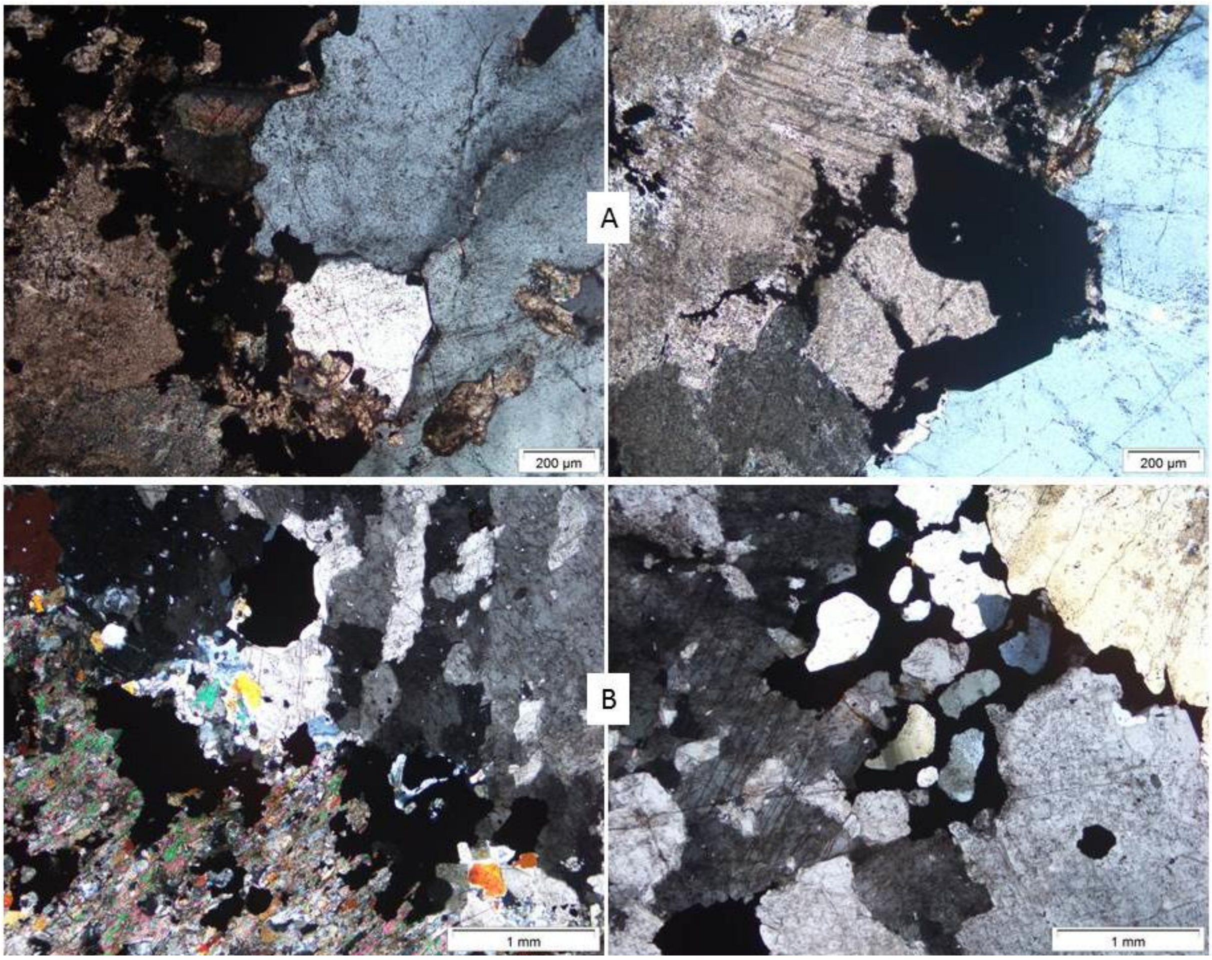

Figure 5.7: Thin section microphotographs in XPL from borehole KM12-01 of the Kariam Prospect. A) Quartz-carbonate veins consists of quartz with undulose extinction and grains are fractured, twinned carbonates and sulphides, at depth 30 m. B) Sulphide mineralised quartz-carbonate vein hosted in a carbonate biotite rich schist. A clear contact between the mineralised quartz-carbonate vein and the host quartz biotite is observed, at depth 45.8 m.

Samples in figure 5.6 and 5.7 represent mineralised quartz and carbonate veins from the Kariam Prospect. These veins are hosted by the bleached-quartzitic unit (quartz-carbonate schist). Sample 5.7A represents a sulphide mineralised carbonate-quartz vein. This sample consists of approximately 70 % of carbonate minerals mostly grainy calcite with high birefringence and clear twins. The coarse quartz grains display an undulose extinction which indicates possible stress and the grains are fractured. The carbonates fill the fractures within the quartz grains (Fig. 5.6 and Fig. 5.7A). The sulphides fill fractures in both the quartz and carbonate grains (Fig.5.6 and Fig. 5.7A and B). Quartz grains are in direct contact with the carbonate grains. Clear contacts between the quartz-carbonate veins and the host unit are observed. The boundary is so sharp that there is no evidence of alteration reactions.

Sulphides examined are closely related to the carbonate veins (Fig. 5.6 and Fig. 5.7 A-B). They are also associated with the carbonate minerals within the host rock occurring as disseminated sulphides displaying a weak foliation parallel to the lithological foliation (Fig. 5.7A).

The paragenetic sequence for the sulphide rich sections is quartz -> carbonates -> sulphides.

Ore minerals / Reflected light microscopy

Based on drill core examination two ore types were observed;

i) vein ore, with medium to coarse grained chalcopyrite, pyrrhotite and pyrite and

ii) disseminated chalcopyrite and pyrite within the matrix of the host rocks.

The majority of the primary copper mineralisation in the form of chalcopyrite is associated with the quartz-carbonate veins. The mineralised quartz-carbonate veins are dominantly associated with the bleached halos (quartz-carbonate schists) with minor mineralisation occurring within the chlorite-sericite schist. Generally, the sulphides occur as inclusions, as stringer veinlets, blebs, patches and disseminated. Within host rocks, sulphides occur as blebs sub-parallel to the foliation and disseminated within the matrix of the host rocks proximal to areas around the veins. They also occur at grain boundaries

-Pyrite

Pyrite is observed to occur as euhedral grains within the chalcopyrite grain and within the fine-grained matrix of the host rocks though this is not common (Fig 5.9B). There are small semi rounded pyrite blebs overgrowing the biotite and chlorite. It commonly occurs as disseminated, patches, blebs and veinlets within the veins and within matrix of the host units. It also occurs as inclusion within the chalcopyrite and pyrrhotite grains. The presence of colloform pyrite (red arrow in figure 5.9A) suggests an environment in which pyrite can be replaced (Kuiseb Copper Company, 2013). There are small rounded pyrite blebs overgrow the biotite and chlorite and carbonates.

-Pyrrhotite

Euhedral grains of pyrrhotite, noticeably more inclusion rich than the chalcopyrite and pyrite infills fractures within quartz and carbonates. It is intergrown with chalcopyrite and in places occurs as inclusions within the chalcopyrite grains (Fig 5.5 A and B). It is overgrown by unidentified elongated minerals (Fig. 5.9C and D). It is the dominant sulphide.

-Chalcopyrite

A close association of chalcopyrite and pyrrhotite was observed with chalcopyrite overgrowing the pyrrhotite (Fig. 5.8A-B and Fig. 5.9D) and forming rims within the pyrrhotite grains (Fig. 5.8A). Disseminated grains of chalcopyrite occur as inclusions within the pyrrhotite grains. It also occurs as blebs at grain boundaries of silicate and carbonate grains. Observed to be in in veinlets form and fill fractures.

The sulphide paragenetic sequence as determined from the polished sections appears to be pyrite -> pyrrhotite and chalcopyrite, late pyrite grains are also present.

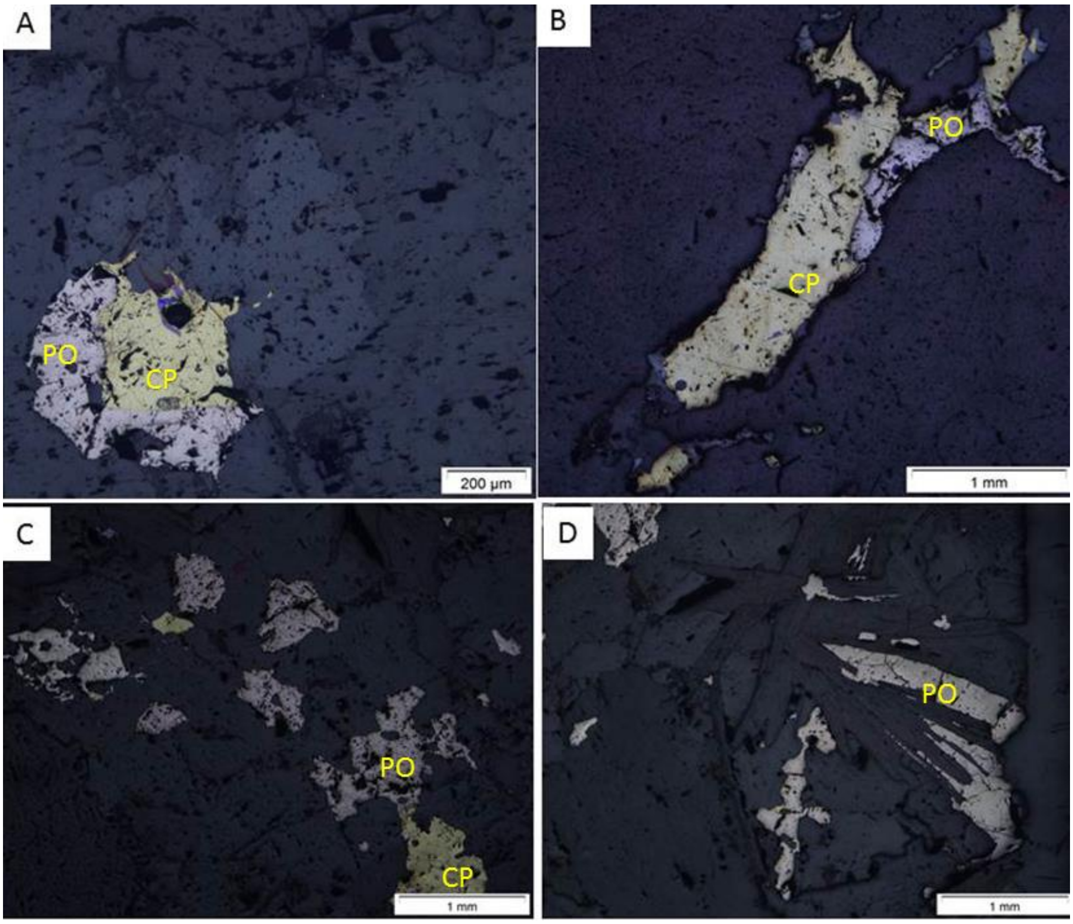

Figure 5.8: Polished section microphotographs from borehole KM12-01 an KM12-02 of the Kariam Prospect in PPL. A) An intergrowth of euhedral chalcopyrite(CP) (yellow) with pyrrhotite(PO) (light pink) at 173.4 m. B) Chalcopyrite and pyrrhotite occurring as veinlets in a fracture, KM12-02 at 143 m C) Patchy and disseminated grains of chalcopyrite and pyrrhotite, KM12-01 at 108.5 m D) Pyrrhotite with a lot of inclusions, note the chalcopyrite occurring as inclusions within the pyrrhotite grains, KM12-01 at 99.4 m.

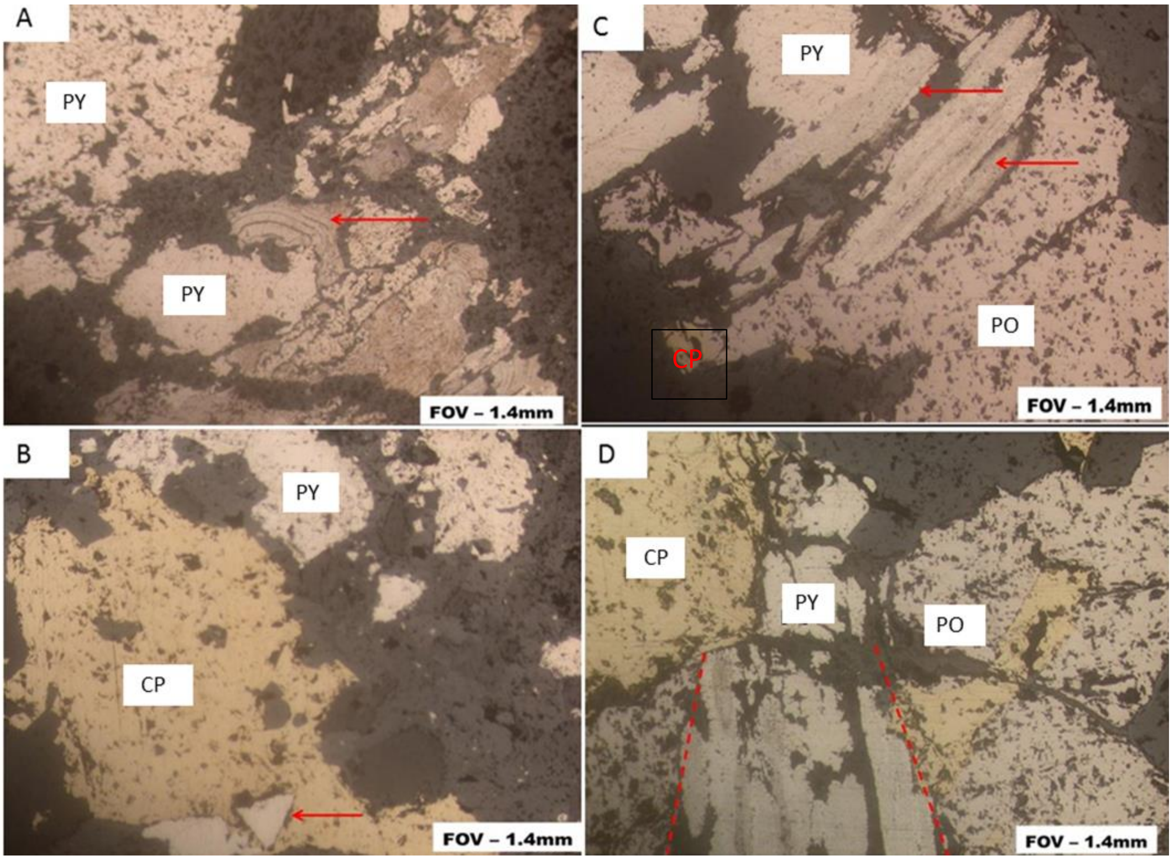

Figure 5.9: Polished section microphotographs from borehole KM12-01 of the Kariam Prospect (Kuiseb Copper Company, 2013). A) Shows pyrite (PY) and note the colloform pyrite shown by the red arrow, depth 30 m. B) Shows chalcopyrite grains (CP) and pyrite (PY). Note the euhedral pyrite grain within the chalcopyrite indicated by the red arrow at depth 30 m. C) Shows pyrite (PY), chalcopyrite (CP) and pyrrhotite (PO). Note the presence of unidentified elongated mineral that overgrowths the sulphides, depth 45.8 m. D) Shows chalcopyrite (CP), pyrite (PY) and pyrrhotite (PO) and an unidentified mineral overgrows the pyrrhotite indicated by red dotted lines, at depth 45.8 m.

CHAPTER 6

DISCUSSION

6.1 Stratigraphy and Structure

The area of study within the Kariam Prospect (EPL 5386) is located north of the Matchless Amphibolite Belt, in the upper part of the Kuiseb Formation of the Southern Zone of the Damara Orogen. Generally, the Kuiseb Formation is made up of successions of quartz-mica schist with subordinate micaceous quartzite, carbonaceous schists, amphibolites (Matchless Member) and calc-silicates with a maximum stratigraphic thickness of about 10km (Killick, 2000). From the transects done, the Kuiseb Formation within the Kariam Prospect is made up of successions of mica-rich and quartz-rich schists interbedded with each other. Kukla et al (1988) interpreted the Kuiseb schists as deposits of an elongated deep-sea fan system indicated by the sedimentary facies and the great lateral extent of the large scale sedimentary cycles traceable for over 100km along the Southern Zone.

The predominant minerals making up the studied schists include quartz, muscovite, carbonate, chlorite, biotite and minor feldspar (albite). Petrographic analyses of thin sections and polished sections show that the veins contain a larger carbonate component than observed in hand specimen. The carbonates have a vuggy texture and are comprised of magnesite, Fe-carbonate (Kuiseb Copper Company, 2013) and calcite. Within the mica-rich schist, biotite and chlorite speckled textured alteration occurs where quartz veining is significant and this is confirmed from field work to be an alteration of the fine-grained, highly foliated mica-rich rock. A late alteration of host rock due to invasion by a very late set of quartz veins is evident as quartzitic zones approximately 4-5 times the width of the intruding vein. The quartzitic zones are comprised mainly of quartz and carbonates and make up the hanging wall and footwall of the late vein.

The Kuiseb schist package in the studied area of the Kariam Prospect has a relative uniform foliation observed to be striking approximately in the ENE-WSW direction, this resembles the regional structure dominated by NE-trending metamorphic foliation and compositional banding observed around the MAM (Shikongo and Hiveluah, 2012). The areas around the MAM are characterized by tight to isoclinal folds and two penetrative cleavages overprinted by a later crenulation cleavage (Fig. 6.1) (Kukla et al, 1988), this was similarly observed in the Kariam core.

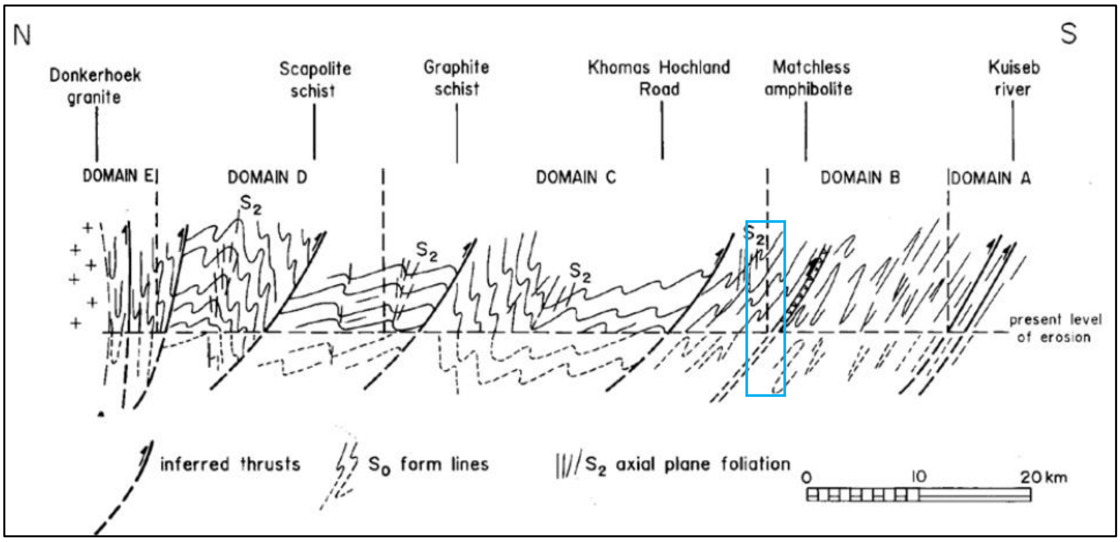

Figure 6.1: Structural profile across the western Southern Zone showing the foliation form lines, D_2 fabrics and inferred thrust zones. The domain boundaries are based on changes in fabric development. Steeping of the S_0 axial planes is observed northward (Kukla et al, 1988). The domain close to area of study is highlighted in blue.

The ENE-WSW mica schists preserve a strong, penetrative metamorphic cleavage defined by the parallel orientation of the fine-grained muscovite and a second set of foliation defined by the acicular biotite orthogonal to the fine-grained foliation. Crenulation cleavage, crenulation folding and faults identified indicate different deformational episodes/events. There must have been extensional event that resulted in thicker quartz-carbonate veins. Based on vein mapping, two different orientations were identified; the ENE-SWS set parallel to lithological foliation along predisposed weaknesses and this is attributed to an early deformational event. The late set of quartz veins linked to the latest deformational even in the study area is orthogonal to the lithological foliation. These two quartz sets indicate that two or more hydrothermal activities have occurred in the area.

6. 2 Mineralisation

Breitkopf and Maiden (1988) described the deposits along and around the MAB to be massive to semi-massive pyritic copper deposits and sporadically developed in clusters along the belt (Fig. 2.5) with orebodies deformed to cigar or pencil shapes. Although every cluster of deposit has its own characteristics, there are many similarities from one to the other. Characteristic features of volcanic massive sulphide deposits are as follows; comprising largely massive ores of pyrite with lesser amounts of chalcopyrite and pyrrhotite with the mineralisation predominantly stratiform and conformable to bedding (Killick, 2000).

Mineralisation within the studied core from the Kariam Prospect includes pyrrhotite as the dominant ore mineral, pyrite, magnetite, chalcopyrite hosted by the quartz-carbonate veins with molybdenite occurring locally as an accessory phase. Disseminated and patchy sulphides were observed within host rocks in areas proximal to the mineralised veins (Fig. 5.7). The presence of carbonate in rocks hosting the mineralised veins explains the possibility of sulphide transportation along with the carbonate resulting in a simultaneously precipitation. In some areas, the contact between the mineralised veins and the host rock are sharp with little or no evidence of alteration reactions or chemical exchange between them (Fig. 5.8 and Fig. 5.9). At Kariam Prospect, the upper sections of the boreholes are more oxidised, consisting of chalcopyrite, pyrite, magnetite and molybdenite and the lower sections are weakly oxidised with chalcopyrite, pyrite and pyrrhotite.

From soil geochemistry, high copper values correlate with magnetic data (Fig. 3.3 and Fig. 3.4) with high magnetic values associated with quartz veins enriched with magnetite (as observed from the field) and oxidised pyrrhotite. Based on the sun-shaded terrain model image with an overlay of the gridded Cu values (Fig. 3.3), the Cu anomalism and topography are strongly controlled by the NNE structural direction, with the section A-B showing the strongest Cu anomaly at elevations between 1600 m and 1700 m above mean sea level (Kuiseb Copper Company, 2013). It was interpreted by Kuiseb Copper Company (2013) as exposed supergene enrichment relating to a paleo-surface and may explain the lack of anomalous Cu associated with the magnetic anomalies in the SE (deeply eroded) and the NW (not eroded sufficiently) which however does not explain the Cu anomalism on the NE side (Fig. 3.3). It is also likely that the difference in topographic elevation is irrelevant, and maybe it has to do with fluid migration paths availability.

The mineralised vein system is orthogonal to the host-rock foliation and occurs as an extensional vein set and controlled by an unidentified structure trending WNW-ESE (Fig. 3.3). The presence of high amount of alteration suggests that a greater volume of fluids went through these rock units. The presence of magnetite indicates that the alteration processes were of an oxidizing nature.

The deposits associated with the Matchless Member have many traits of volcanic-hosted massive sulphide deposits, however only few of these deposits have volcanic hosts and the Kariam mineralisation is part of those lacking a volcanic host. The mentioned features are however not present within the selected area of study. The Kariam Prospect hosts a vein-hosted style of mineralisation.

Additionally, the majority of the MAM deposits have similar characteristics as the Besshi-type deposits of Japan which Yui (1983) and Fox (1984) pointed out to have the following features; they comprise largely of massive ores of pyrite with lesser amounts of chalcopyrite and pyrrhotite with the mineralisation predominantly stratiform and conformable to bedding. Moreover, the deposits are products of basic submarine volcanism within the thick sequences of the continentally-derived clastic sediments with graphic argillite commonly present and carbonate may be associated with the deposit. They are observed to be confined to a definite stratigraphic zone.

Table 5: Comparison of general features of the Kariam copper, Onganja copper and Matchless copper with reference to Karsch (1983), Moore (2010) and Killick (2000).

	Kariam	**Onganja**	**Matchless**
Host sequence	Kuiseb Formation	Kuiseb Formation	Kuiseb Formation
Host rocks	Quartz-carbonate schists	Quartz-plagioclase-biotite schist	Sericite-quartz schist, mica schist, amphibolite schist, amphibolite
Metamorphism	Amphibolite facies	Amphibolite facies	Amphibolite facies
Mineralisation setting	Orthogonal high-angle quartz-carbonate veins	Sheeted-vein complex, orthogonal high-angle extensional veins	Massive and semi-massive sulphides
Vein description	2 vein sets, medium-coarse grained, thickness reaches > 3m, late carbonate	Single-stage, single vein set, very coarse-grained, thickness attains >5m, late carbonate brecciation	veinlets or sulphide-bearing quartz-carbonate veins
Ore paragenesis	Pyrite-pyrrhotite-chalcopyrite-magnetite-molybdenite	Pyrite-chalcopyrite-molybdenite-magnetite-native gold	Pyrite-pyrrhotite-chalcopyrite-sphalerite
Metal association	Cu (-Mo-Au)	Cu (-Mo-Au)	Cu-Zn (-Ag-Au)
Alteration assemblage	Proximal: quartz-carbonate-sericite-chlorite Distal: chlorite-biotite	Proximal: albite-chlorite-carbonate-muscovite-albite Distal/early: Cl-rich biotite-scapolite	Chlorite-sericite

Gangue	Quartz-carbonate	Quartz-calcite-apatite	Quartz-calcite-apatite

The alteration of the host rock of Kariam is comparable to the alteration of the quartz-plagioclase-biotite schist in contact with the mineralised veins of the Onganja deposit (Moore, 2010) (Table 5). The alteration in Onganja is more scapolite-biotite on the outer zone with albite particularly with the carbonate veins (Moore, 2010), while the Kariam alteration is mainly biotite-sericite on the outer zone with carbonate and minor albite close to the quartz-carbonate mineralised veins. In both Onganja and Kariam Prospect, mineralisation is associated with steeply dipping quartz-carbonate veins, with both veins orthogonal to host-rock foliation., Onganja assemblage is more oxidised and has chalcopyrite, pyrite, magnetite and molybdenite (Moore, 2010), this is similar to the mineral assemblage with additional pyrrhotite which is found in the Kariam prospect (Table 5).

Ideally, a VMS deposit should consist of two parts, a concordant massive sulphide lens with > 60% sulphides and a discordant vein-type sulphide mineralisation located mainly in the footwall strata, known as the stockwork (Fig. 6.2).

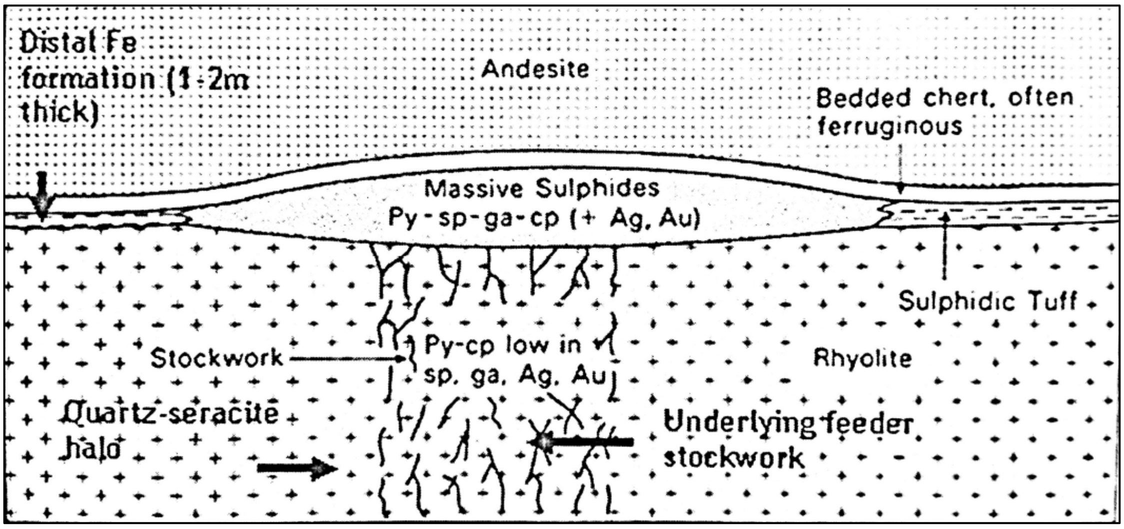

Figure 6.2: Shows a general VMS model from Evans (1993). No massive sulphide component was observed from the available Kariam data.

Although the Kariam Prospect is located close to a known VMS Matchless deposit (Otjihase and Matchless deposits), the available data point it to a vein-hosted type of deposit because of the absence of massive to semi-massive sulphides. However, despite the lack of massive ore in studied core, massive copper mineralisation is stated to be present within the Hureb Prospect, 30 km north of the Kariam Prospect (Kuiseb Copper Company, 2013). Could this be part of the package or totally a different type of mineralisation? What is the relationship between the two styles of mineralisation? These are the questions that need answers and can only be answered through additional work in the area.

From the available data, it is possible that the Kariam mineralisation is genetically different from the other deposits within the Matchless Belt. It is possible that the mineralisation hosted in the Kariam Prospect is like some deposits hosted by the Kuiseb Formation schists i.e. Onganja copper-gold mineralisation. Another possibility is that the Kariam mineralisation represents a distal part of the VMS system along the MAM.

CHAPTER 7

CONCLUSION

The Kuiseb Formation package in the Kariam Prospect is represented by altered quartz and mica schists with variable amounts of quartz, carbonates, biotite, chlorite, muscovite and minor feldspars with the dip approximately 60° to the NW. Different sets of quartz and carbonate veins are observed; (i) quartz veins striking ENE-WSW, (ii) gossanous quartz carbonate veins orthogonal to the lithological foliation with a NNE-SSW strike and tiny folded quartz. The ore minerals which occur within the studied area include oxides (magnetite), pyrrhotite, chalcopyrite, pyrite and molybdenite.

The two borehole cores demonstrate that sulphides, at least locally, are concentrated but not restricted to the veins within the quartz-carbonate schist and minor amounts in veins within the sericite chlorite schist. Mineralisation is also present in the matrix proximal to the post tectonic veins. The dominant styles of mineralisation include disseminated, veinlets, blebs and patchy occurrences. The mineralised veins show little to no alteration other than weak silicified halos. Alteration can be broadly divided into an outer biotite chlorite zone and the inner quartzitic zone, particularly in association with most the mineralised quartz-carbonate veins. Overall, the Kariam mineralisation is vein hosted, proved by the available ground magnetic, soil sampling and field data.

The following is recommended for future work:

- Drill more boreholes in the area to help establish the mineralisation vector.
- Additional geological mapping to produce a combined map of the Kariam and Hureb Prospect and examine their relationships, if any.
- Conduct geological work and mineral exploration around the MAM within the Kariam Prospect and the Hureb Prospect.
- Conduct Re-Os for dating sulphides to compare to mineralisation dates with the Matchless, Otjihase deposits and the Onganja mineralisation and possibly Navachab Mine.
- Conduct stable isotope work on pyrite, chalcopyrite and calcite and compare with existing data from Matchless and Otjihase deposits.

CHAPTER 8: REFERENCES

Barnes, S.J. 1982. Serpentinites in central South West Africa/ Namibia - a reconnaissance study. Memoir, Geological Survey of South West Africa, Namibia, 8,90pp.

Breitkopf, J.H and Maiden, K.J., 1988. Tectonic Setting of the Matchless Belt Pyritic Copper Deposits, Namibia. Economic Geology. 83, 710-723.

Coward, M.P. 1983. The tectonic history of the Damaran belt. Special Publication, Geological Society of South Africa. 11, 409-421.

de Kock, G.S., 1989. *´n Geotektoniese studie van die Damara-orogeen in ´n gebied suidoos van Karibib, Suidwes-Afrika*. Unpublished Ph.D. thesis.

Evans, A., 1993. Ore Geology and Industrial Minerals. 3rd Ed. The Continental crust and its Mineral Deposits. Geological Association of Canada. Special paper 20, 109.

Fox, J.S. 1984. Besshi-type volcanogenic sulphide deposits – a review. CIM Bull., 77, 57-68.

Frimmel, H.E., Basei, M.S. and Gaucher, C. 2011. Neoproterozoic geodynamic evolution of SW-Gondwana: A Southern African perspective. International Journal of Earth Sciences, 100, 323 - 354.

Gray, D.R., Foster, D.A., Meert, J.G., Goscombe, B.D., Armstrong, R., Trouw, R.A.J., Passchier, C.W., 2008. A Damaran Perspective on the Assembly of Southwestern Gondwana. Geological Society of London Special Publication.

Hawkesworth, C.J., Kramers, J.D., Miller, R., 1981. Old model Nd ages in Namibian Pan-African rocks. Nature 289, 278 – 282.

Kasch, K.W., 1983. Continental collision, suture progradation and thermal relaxation: a plate tectonic model for the Damara Orogen in central Namibia. Special Publication, Geological Society of South Africa .11, 423-429.

Killick, A.M., 1983. Sulphide mineralization at Gorob and its genetic relationship to the Matchless Member, Darnara Sequence, SWA/Namibia. Special Publication, Geological Society of South Africa.11, 381-384.

Killick, A.M., 2000. The Matchless Belt and associated sulphide mineral deposits, Damara Orogen, Namibia. Communications of the Geological Survey of Namibia. 12, 79-87.

Klemd, R., 1987. The Matchless copper deposit, South West Africa/Namibia a deformed and metamorphosed massive sulfide deposit. Economic Geology. 82, 587–599.

Klemd, R., Maiden K.J. and Okrusch, M., 1987. The Matchless copper deposit SWA/Namibia: A deformed and metamorphosed massive sulfide deposit. Economic Geology.82, 163-171.

Klemd. R., Maiden. K. J., Okrush. M and Richter, P., 1989. Geochemistry of the Matchless Metamorphosed Massive Sulfide Deposit, South West Africa/Namibia: Wall Rock Alteration during Submarine Ore-Forming Processes. Economic Geology. 84, 663-617.

Kuiseb Copper Company (Pty) Ltd. 2013. Renewal report for Exclusive Prospecting License 3899, Windhoek District., Khomas Region.

Kukla, P.A., 1992. Tectonics and Sedimentation of a late Proterozoic Damaran convergent continental margin, Khomas Hochland, Central Namibia. Memoir Geological Survey of Namibia **12** pp95.

Kukla, P.A. and Stanistreet, I.G.,1991. The record of the Damaran Khomas Hochland accretionary prism in Central Namibia: refutation of an "ensialic" origin of a Late Proterozoic orogenic belt. Geology, 19, 473-476.

Kukla, P.A., Stanistreet, I.G., and Henry, G., 1991. Sedimentary basinal responses to a late Precambrian Wilson Cycle: the Damara Orogen and Nama Foreland, Namibia. Journal of African Sciences. 13 (1), 141-156.

Kukla, P.A., Opitz, C., Stanistreet, I.G. and Charlesworth, E.G. (1988). New aspects of the sedimentology and structure of the Kuiseb Formation in the western Khomas Trough, Damara Orogen, SWA/Namibia. Communications at Geological Survey of Namibia, 4, 33-42.

Miller, R.M.G., 1983. Evolution of the Damara Orogen of South West Africa/Namibia. Special Publication, Geological Society of South Africa. 11.

Miller, R.M.G., 2008. The Geology of Namibia. Volume 2: Neoproterozoic to Lower Palaeozoic. Geological Survey of Namibia, Windhoek, Namibia. 320.

Moore, J.M., 2010. Comparative study of the Onganja Copper Mine, Namibia: A link between Neoproterozoic Mesothermal Cu (-Au) mineralisation in Namibia and Zambia, South Africa Journal of Geology, 113, 445-460.

Schneider, G.I.C., and Seeger, K.G., 1992. The Mineral Resources of Namibia. Geological Survey of Namibia.118.

Shikongo, J. and Hiveluah, H. 2012. Mine review: A brief description of the Matchless Mine. Internal report for the Matchless Mine, 12 pages.

Yui, S. 1983. Textures of some Japanese Besshi-type ores and their implications for Kuroko deposits. Economic Geology. 5, 231-240.

APPENDIX 1

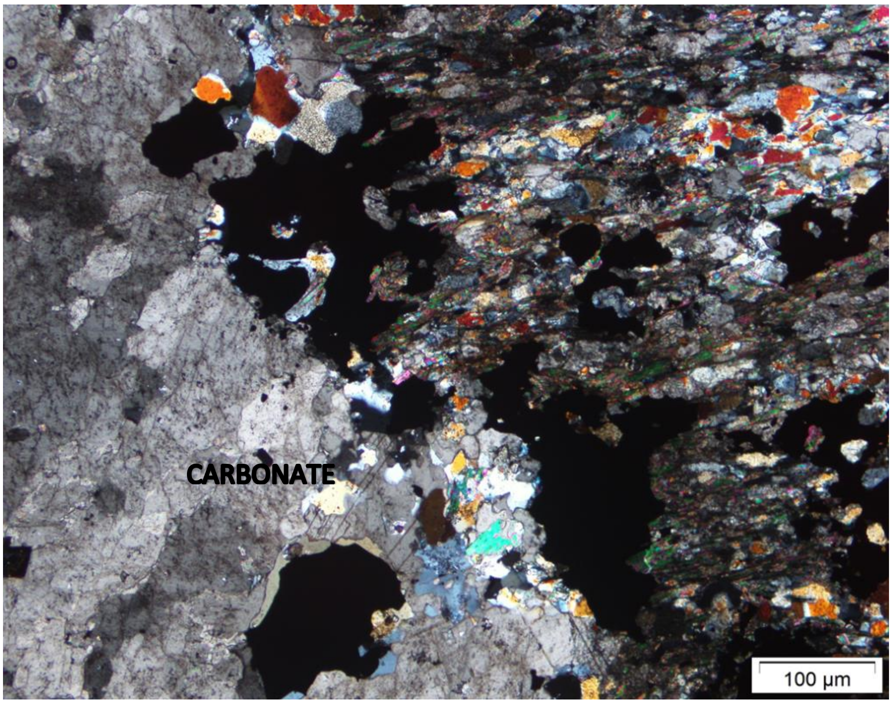

Figure 9.1 Thin section microphotograph showing the contact between the carbonate-quartz and the host rock. Sulphides present in the carbonate veins and carbonate within the host rock, KM12-01 at 45.8 m.

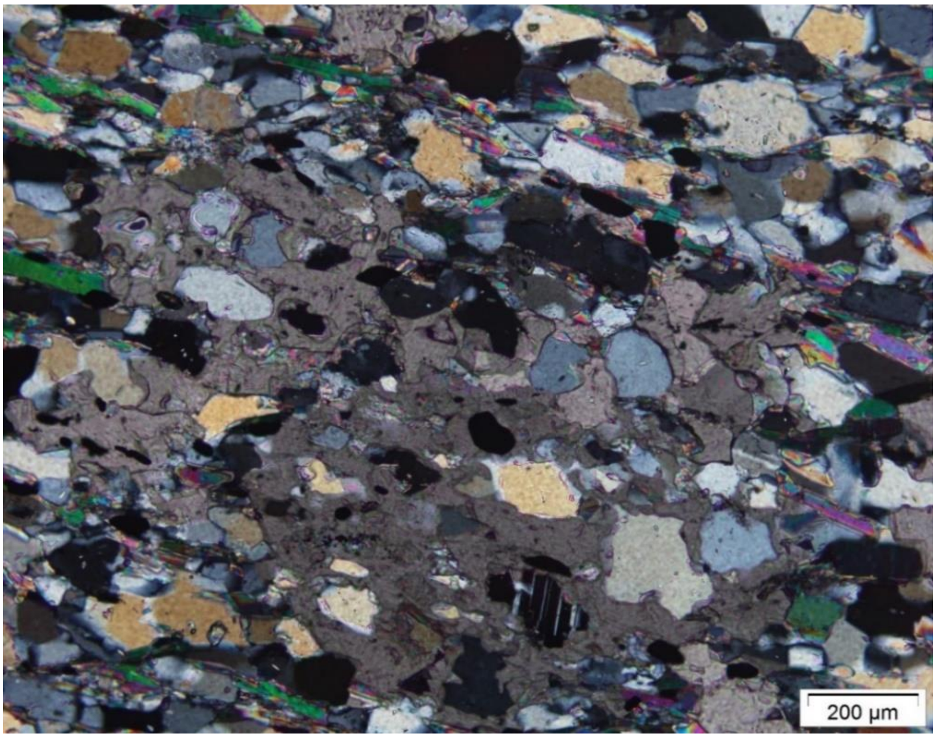

Figure 9.2: Thin section microphotograph of a quartz-carbonate schist. Dominant minerals include quartz and carbonate with minor muscovite and trace amount of feldspars (albite), KM12-01 at 109.78m

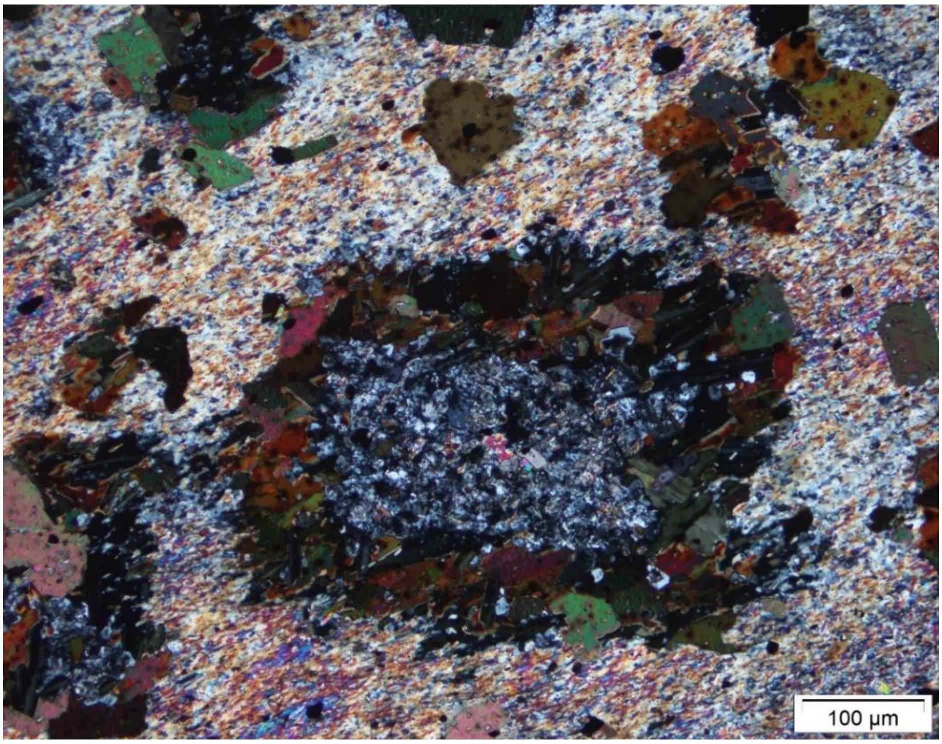

Figure 9.3: Thin section microphotograph of a biotite-chlorite schist. Shows the cluster of zoned quartz, biotite and chlorite in a fine-grained sericite/muscovite matrix. Individual biotite and chlorite grains float within the matrix too, KM12-02 at 112 m.

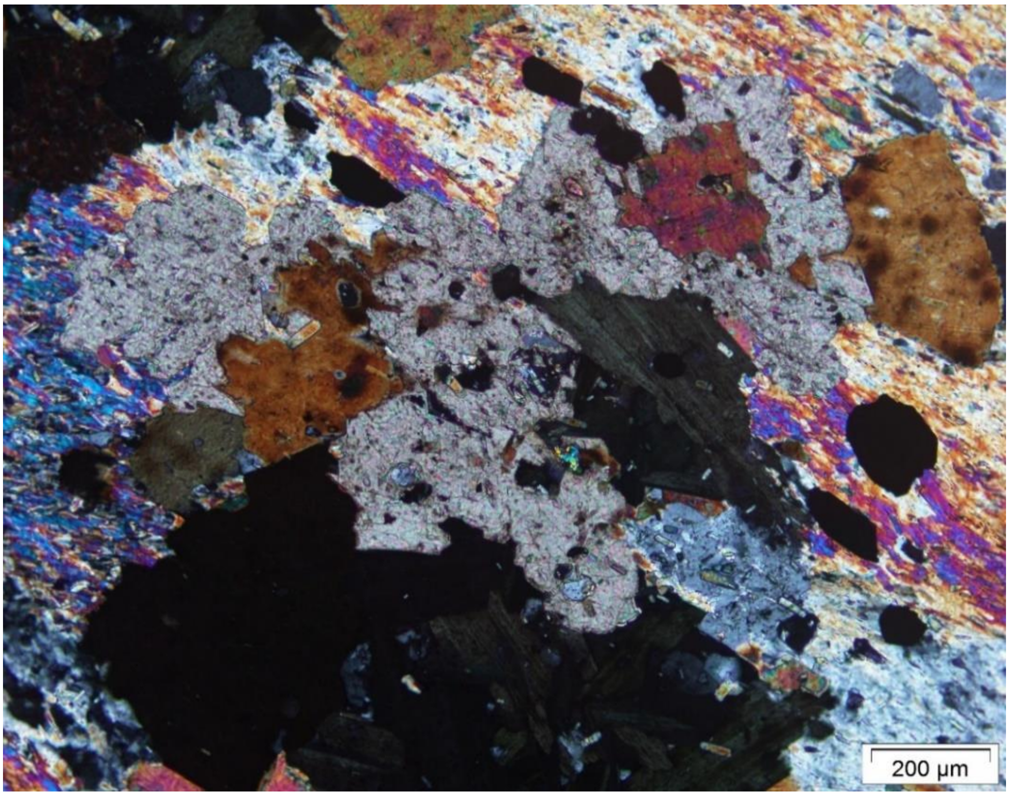

Figure 9.4: Thin section microphotograph of the biotite-chlorite schist of the Kariam Prospect. Shows the fine-grained matrix with biotite, chlorite and vuggy carbonate minerals, KM12-01 at 173 m.

APPENDIX 2

Table 5: Logging dictionary used for the Kariam drillcore.

Lithologies		Minerals		Mineral location		Mineralisation style		Texture	
Code	Description	Code	Description	Code	Description	Code	Description	Code	Description
BCS	Biotite-Chlorite schist	AB	Albite	MTX	Matrix	di	disseminated	ac	acicular
BS	Biotite schist	BT	biotite	VNS	Veins	pa	patchy	eu	euhedral
MS	Muscovite schist	CH	chlorite			ve	veined	ma	massive
CSS	Chlorite-Sericite schist	MT	magnetite					sp	speckled
UDL	Undifferentiated unit	MU	muscovite					pk	poikilitic
		QZ	quartz					sc	schistose
		CA	carbonate						
		CL	calcite						
		CP	chalcopyrite						
		MO	molybdenite						
		PO	pyrrhotite						
		PY	Pyrite						
		SE	sericite						
		Structural logs		Alteration		Alteration style			
		Code	Description	Code	Description	Code	Description		
		bo	boudin	bl	bleaching	sp	speckled		
		cr	crenulation	cl	chlorite	ma	massive		

				fo	foliation		bt	biotite		fo	foliation				
				Fr	fracture		se	sericite							
				sh	shearing										

APPENDIX 3

This Appendix provides details of the borehole core logging for the two boreholes KM12-01 and KM12-02 which are shown graphically in Figure 4.12

Table 5: Geological log for borehole KM12-01 of the Kariam Prospect

Azimuth: 318° Easting: 6579978

Dip: -60° Northing: 7484463

EOH: 399. 15 m

m From	m To	Litho Code	Texture				Mineralisation and style						Location	Alteration and style		Comments
0	23.3	MRS	fo			Py						di, ve	VNS			Quartz and carbonate veins, intensely fractured (fr)
23.3	66.2	BCS	sp	fo	ma	Py	Mt	Cp	Mo	Po		di, ve, pa	VNS, MTX	bi-cl, bl	sp, ma	Quartz veins cross cutting foliation enriched in sulphides, magnetite within the matrix of the bleached halo, local shearing at around 58m, couple of barren veins.
66.2	70.2	BS	ma	fo												massive, very minor foliation, competent layer, minor fracture, very little quartz veins and possible albite
70.2	71.4	BCS	sp	fo	Ve									bi-cl, bl	sp, ma	Barren quartz veins
71.4	72.9	BS	ma													Rarely foliated
72.9	82.8	BCS	sp			Py	Po	Cp				ve, pa	VNS, MTX	bi-cl, bl	sp, ma	local shearing at 75.6-77.9m, quartz veins with Po, Cp and minor Py. 77m quartz vein parallel to foliation with very minor Py, most if not all the quartz veins close to the shear zones are barren.
82.8	91	CSS	fo	ve		Py						ve, pa	VNS	se, cl	ma, fo	Barren quartz veins parallel to foliation
91	94.7	BCS	sp	fo		Py	Cp	Po	Mo			pa, ve	VNS	bi-cl, bl	sp, ma	Intermediate foliation, Py, Po, Cp in the quartz veins cross cutting the foliation and barren quartz vein parallel to foliation
94.7	99.4	BS	ma													Hardly foliated with quartz veins of >1mm
99.4	106.8	BCS	sp	fo		Py	Po	Py	Mt?			pa, ve	VNS, MTX	bi-cl, bl	sp, ma	Milky quartz vein with Cp, Po, Py. Locally sheared with barren quartz veins. Magnetite in the matrix of the bleached halo

106.8	109.2	BS	ma			Py	Cp					Pa	VNS			A thin quartz vein with Py and Cp
109.2	114.5	BCS	sp			Cp	Py	Po	Mt?			ve, di, pa	VNS, MTX	bi-cl, bl	sp, ma	More Mt, Cp, Po, Py within the bleached unit, carbonate vein at 112.6m with Py
114.5	119	BS	ma	fo												whitish minerals (albite?), competent unit.
119	131	BCS	sp	fo		Cp	Py	Po	Mt?			ve, di, pa	VNS, MTX	bi-cl, bl	sp, ma	locally shearing (sh), intense foliation, quartz veins with Cp, Po, Py, Mg
131	138	CSS	fo	ve		Po	Cp					ve, pa	VNS	se, cl	ma, fo	Po rich quartz veins, intense foliation, minor Cp bleb within a 10cm quartz vein, intense veining.
138	142.9	BS	ma													Barren quartz veins
142.9	165	CSS	fo	ve		Po	Cp	Py				ve, pa	VNS	se, cl	ma, fo	Bleached unit with Cp, Po, Py within the clear/milky quartz veins, foliation, gossanous quartz veins with sulphides at around 148.8m -149.1m.
165	168.5	BCS	sp	ma		Py							VNS	bi-cl, bl	sp, ma	Minor Py, many tiny barren quartz veins
168.5	172.1	BS	ma			Po	Mt?					Di	VNS, MTX			
172.1	177.4	BCS	sp	fo		Po	Cp	Py	Mt?			ve, pa, di	VNS	bi-cl, bl	sp, ma	Cp, Py, Po, (Mt) in veins within the bleached unit.
177.4	180	BS	ma													Minor foliation
180	187.8	CSS	fo	ve		Py						Pa	VNS	se, cl	ma, fo	Patchy Py in the quartz vein, locally sheared (sh)
187.8	192.8	UDL	fo	sp	ma											Combination of BS, BCS and CSS. Barren quartz veins
192.8	203	BCS	sp											bi-cl, bl	sp, ma	Foliated, barren quartz veins, minor sericite
203	209.2	UDL				Py						pa	VNS			Combination of BS, BCS and CSS.
209.2	215	BCS	sp			Py	Po	Cp	Mo			ve, pa, di	VNS	bi-cl, bl	sp, ma	Quartz veins parallel to foliation
215	219.7	CSS	fo	ve										se, cl	ma, fo	Foliated, barren quartz veins, minor sericite
219.7	224.5	BS-BCS	ma	sp										bi-cl	sp	Quartz veins >1mm parallel to foliation
224.5	244	BCS	sp	fo		Py	Po	Cp				ve, pa, di	VNS	bi-cl, bl	sp	Quartz veins
244	252.2	UDL				Py						ve	VNS			Combination of BCS, BS and CSS
252.2	255.4	BS	ma													

255.4	265	CSS	fo	ve		Po	Py	Cp				pa, ve	VNS	se, cl	ma, fo	Carbonate-quartz vein with Py, Po and Cp
265	296.95	BS	ma	fo		Cp	Po	Py				pa, ve	VNS			Quartz veins
296.95	319	BS-CS	fo													Barren quartz veins
319	363.3	BCS	sp	fo										bi-cl, bl	ma, sp	Quartz veins
363.3	390.3	BS	ma													
390.3	399.15	BCS	sp			Py						ve, pa	VNS	bi-cl, bl	ma, sp	Quartz veins with pyrite between 397.3m - 399.15

Table 6: Geological log for borehole KM12-02 of the Kariam Prospect.

Azimuth: 305° Easting: 656348

Dip: -60° Northing: 7484923

EOH: 302.45 m

m From	m To	Litho Code	Texture			Mineralisation and style					Location	Alteration and style		Comments
0	2.59	RSO												Top soil with quartz fragments
2.59	16.5	MRS	fo											Biotite and muscovite rich schist, iron rich-vugs, foliated, barren quartz veins parallel to foliation, brown carbonate veins
16.5	47.7	BCS	sp	fo		Mt	Po	Py	Cp	ve, pa	VNS, MTX	bi-cl, bl	sp, ma	Local folding at 29.3m, 1.3m bulky quartz-carbonate vein hosting the sulphides at around 29.6m - 30.9m. 30cm quartz vein enriched in Py at 36m - 36.3m.
														<1cm quartz vein at 45.2m enriched in sulphides, Bleached halo rich in magnetite
47.7	50.7	BS	ma											Up to 1cm barren quartz veins
50.7	54.7	BCS	sp	ma		Po	Cp					bi-cl, bl	sp, ma	Up to 1cm quartz veins
54.7	56	BS	ma											
56	61	BCS	ma	sp		Po	Cp	Py		ve, pa	VNS	bi-cl, bl	sp, ma	50cm thick quartz vein

61	67.3	BS	ma											Whitish mineral possibly albite, minor foliation
67.3	70.57	BCS	sp	ma	fo	Po	Cp	Py	Mo	ve, pa	VNS, MTX	bi-cl, bl	sp, ma	About 2m of the speckled unit and the rest is made up of the quartzitic/bleached schist
70.57	72.4	BS	ma											
72.4	93	BCS	sp	ma	fo	Po	Cp	Py		ve, pa	VNS	bi-cl, bl	sp, ma	Quartz veins of up to 40cm thick
93	98.8	BS	ma	ve										1mm quartz veins
98.8	102	BCS	sp	ma		Po	Cp			ve, pa	VNS	bi-cl, bl	sp, ma	minor pelitic schist
102	110	BS	ma											Barren quartz veins, minor foliation
110	111.6	BCS	sp	ma		Po	Cp			pa	VNS	bi-cl, bl	sp, ma	1cm quartz vein cross cutting foliation
111.6	114.5	BS	ma											Barren quartz veins
114.5	144	BCS	sp	ma		Po	Cp	Mo		pa	VNS	bi-cl, bl	sp, ma	1 meter thick quartz vein enriched with sulphides in addition to barren quartz-carbonate veins
144	152.3	CSS	fo			Cp	Po	Py		pa, ve	VNS	se, cl	fo	Barren quartz veins cross cutting foliation, however there is a 30cm wide vein hosting sulphides between 149.45m - 149.75
152.3	165	BCS	sp	ma								bi-cl, bl	sp, ma	Chlorite and biotite speckles within a fine-grained sericite matrix
165	201.7	BS	ma											Quartz veins parallel to foliation, whitish mineral possibly albite
201	206	CSS	fo									se, cl	fo, ma	Barren quartz veins
206	215.7	BS	ma											fine gained, dark grey

215.7	220	CSS	fo									se, cl	fo, ma	
220	224.5	BS	ma	fo										Fine grained, dark grey
224.5	230.5	CSS	fo									se, cl	fo, ma	Tones of barren quartz veins
230.5	262.2	BS	ma											Local folding at 238.3m
262.2	264.1	BCS	sp	bl								bi-cl, bl	sp, ma	Barren quartz veins
264.1	270	CSS	fo									se, cl	fo, ma	
270	290.5	BS	ma											Fractured
290.5	295.7	CSS	fo			Cp	Po	Py		pa	VNS	se, cl	ma, fo	Containing a prominent quartz vein
295.7	302.5	BS	ma			Po								Minor quartz veins

APPENDIX 4

Table: 7 Summary of the different rock units identified from the Kariam Prospect

Rock name	Core/field photographs	Thin section photographs	PTS Scans		Descriptions
Biotite chlorite schist		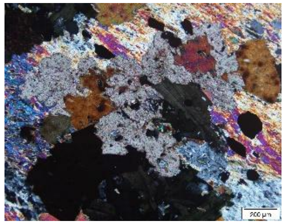			Chlorite biotite clusters rich schist with minor carbonates and feldspars. Local shearing, consists of veins parallel to foliation. It is an alteration product related to the invasion of quartz veins into the muscovite rich schist.
Chlorite sericite schist					Consists of chlorite, sericite (muscovite), biotite and bulky quartz veins. Boudins present, but not common. Minor chalcopyrite within the quartz veins. Medium and coarse grained quartz grains.

Muscovite schist		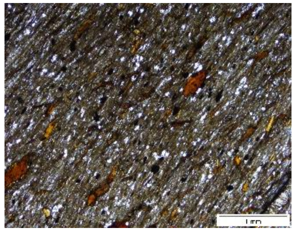			Intensely foliated mica rich schist. Dominated by muscovite with fair amounts of chlorite and biotite. Displays two sets of foliations (I, defined by the fine-grained muscovite and ii, defined by the acicular biotite sub parallel to the muscovite grains). Minor disseminated pyrite present in the matrix.
Quartz carbonate schist		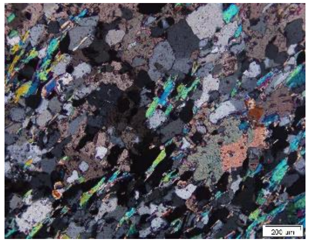			Dominated by quartz and carbonate minerals with minor muscovite and feldspars (albite). Weak foliation displayed by the quartz and muscovite grains. Hosts quartz-carbonate veins with Cp, Py, Po and Mo. Cp and Py in areas proximal to the veins. Believed to be an alteration product resulting from late hydrothermal fluids invasion. Main host for the mineralised quartz-carbonate veins.